Evaluation of a Rapid and Automated Surrogate Virus Neutralization Test in Comparison to a Pseudovirus and Live Virus Neutralization Assay

By

Danielle Ali

B.S. Biological Sciences (Florida International University) 2011

THESIS

Submitted in partial satisfaction of the requirements for the degree of

MASTER OF SCIENCE

in

BIOMEDICAL SCIENCE

in the

GRADUATE SCHOOL

of

HOOD COLLEGE

May 2022

Accepted:

Ann L. Boyd, Ph.D. Committee Member	Ann L. Boyd, Ph.D. Director, Biomedical Science Program
Linwood H. Johnson Committee Member	
Darci R. Smith, Ph.D. Thesis Adviser	April M. Boulton, Ph.D. Dean of the Graduate School

STATEMENT OF USE AND COPYRIGHT WAIVER

I authorize Hood College to lend this thesis, or reproductions of it, in total or part, at the request of other institutions or individuals for the purpose of scholarly research.

DISCLAIMER

The views expressed in this article reflect the results of research conducted by the author and do not necessarily reflect the official policy or position of the Department of the Navy, Department of Defense, nor the United States Government.

DEDICATION

I dedicate my thesis work to my Lord and Savior, Jesus Christ, for getting me through the countless nights when it was just us. I saw your mighty hand move in this journey from start to finish and my faith has reached a new level. I love you, Jesus. For my strong father and beautiful mother, Hugh and Denise, your strength, prayers, and wisdom did not go unnoticed and is what I held onto during the tough moments, and for that, I thank you both. Daddy, I have always admired your work ethic and perseverance in whatever you set out to do. You instilled in my sisters and me the value of education and provided us with the tools we needed to succeed. Mommy, thank you for your sacrifice, sound advice, and always pointing me back to the Lord. Your prayers and encouragement have blessed me immensely. To my late grandmother, (Mumsie), you always cherished the letters I would write to you as a little girl, sharing all of my biggest accomplishments, and I know this one in particular would have brought you so much joy. I know my late Aunt Dorchelle, a teacher who valued education and always supported me, would be so proud of me for this academic achievement. My late Aunt Debra, your favorite and our family scripture, Proverbs 3:5-6, is what pushed me through and propelled me to finish the assignment. To my three intelligent and beautiful sisters, Dionna, Dasha, and Deneria, collectively and individually, you each used your strengths and encouragement to support and lift me up, and I am forever grateful. My loving, patient, and supportive significant other, Jefferson, your push and drive for yourself has always inspired me to do and be better, especially during this experience, and I truly appreciate you. To my godson Julius, I hope to inspire you to always complete your goals and go after your dreams. To my inner circle, Gisaidy, Cynthia, Cedrine, and Samantha,

thank you all for just being there and always checking on me, especially when I was swamped with work. You guys never failed to reach out and it was so needed. To my study group, Jilcia, Luis, and Kenneth, we all know the real deal! It was no easy feat, but we studied together and kept one another encouraged until the end.

Thank you to my extended family, friends, former coworkers, Candice and Clairesa, and countless others who became dear friends, and mentors. Thank you to my church family (the members of the Quinn Chapel African Methodist Episcopal Church) and the overall church community for your prayers and encouragement along the way. It truly took my entire village to get me to where I am today, and I love you all!

"Intelligence plus character – that is the goal of true education."-Dr. Martin Luther King Jr.

ACKNOWLEDGEMENTS

I would like to thank my committee members: Dr. Darci Smith, Dr. Ann Boyd, and Linwood Johnson who offered their expertise, training, and overarching support. Thank you Linwood aka Woody, my project mentor, for always taking the time to explain concepts, ideas, and training on how to perform the sVNT. Thank you Dr. Boyd for agreeing to be my academic advisor, always lending an ear and answering all of my questions. Lastly but certainly not least, a special and sincere appreciation for Dr. Smith for accepting the role of my thesis advisor and taking on the challenge of a near impossible timeline. Dr. Smith, my sincerest gratitude for your more than generous time and leadership.

I wish to thank my fellow colleagues at the NMRC, Dr. Christopher Singh for technical assistance and Dr. Heather Poeck-Goux for early on analysis assistance and the entire team who offered encouragement and support along the way.

Thank you to Dr. Chris Heger and Francisco Ramirez whom were consultants throughout this entire project for the Simple Plex™ immunoassay platform designed by Protein Simple.

Thank you Dr. Eric Laing and Dr. Edward Mitre from USUHS and PI of the PASS study, PASS healthcare volunteers, Dr. Kevin Schully's Lab (NMRC) for completing the MN and Dr. Carol Weiss's Lab (FDA) for completing the PNA and making this entire project possible.

Finally, I would like to acknowledge that this work was supported/funded by the Coronavirus Aid, Relief, and Economic Security (CARES) Act.

TABLE OF CONTENTS

ABSTRACT

The novel severe acute respiratory syndrome coronavirus 2 (SARS-CoV-2) that causes coronavirus disease (COVID-19) has resulted in roughly 500 million confirmed cases of COVID-19 including an estimated 6 million deaths world-wide, as of April 2022. Vaccines were developed and administered limiting the extent of the pandemic, but with the rise of emerging variants, studies to better understand immune protection against COVID-19 have become a high priority. Neutralizing antibodies represent an important correlate of protection for COVID-19. The cell-based neutralization assays that detect and quantify neutralizing antibody titers use either live virus or pseudotyped viral particles (pseudovirus). Live virus cell-based assays are time consuming and require the use of live SARS-CoV-2 but can be substituted with pseudovirus to avoid requirements for biosafety level (BSL)-3 facilities. This has motivated the development of surrogate SARS-CoV-2 neutralization assays that measure inhibition of the spike (S) protein receptor binding domain (RBD) binding its receptor, human angiotensin converting enzyme 2 (hACE2). The current surrogate virus neutralization tests (sVNTs) are ELISA-based, requiring considerable involvement by laboratory personnel for the multiple washes, incubation steps, and reagent additions as well as a plate reader to generate results. The development of a sVNT performed on an automated and rapid platform could be instrumental in furthering the research and clinical assessment of immune protection against COVID-19. Here we developed and evaluated a sVNT performed on the Simple Plex^{TM} rapid and automated immunoassay platform. The test achieves 100% sensitivity and 99-100% specificity and shows a strong correlation with cell-based assays. This rapid and automated sVNT provides a faster and more easily completed assay for determining SARS-CoV-2 neutralizing antibody titers that can be performed in a BSL-2 laboratory.

LIST OF TABLES

LIST OF FIGURES

LIST OF ABBREVIATIONS

ACE2	Angiotensin-converting Enzyme 2
APC	Antigen Presenting Cells
AUC	Area Under the Curve
BAbs	Binding Antibodies
Biosafety Level	BSL
CARES	Coronavirus Aid, Relief, and Economic Security
CI	Confidence Interval
COVID-19	Coronavirus Disease
CV	The Coefficient of Variation
cVNT	Conventional Virus Neutralization Test
CPE	Cytopathic Effect
Dig	Digoxigenin
DoD	Department of Defense
EC_{50}	Half-maximal Effective Concentration
EC_{80}	80% of Maximal Effective Concentration
ELISA	Enzyme-linked Immunosorbent Assay
FDA	Food and Drug Administration
GNR	Glass Nano Reactors
hACE2	Human Angiotensin-converting Enzyme 2
HCoVs	Human Coronaviruses
HIV	Human Immunodeficiency Virus
His	Histidine
HRP	Horseradish Peroxidase

IC_{50}	Half Maximal Inhibitory Concentration
IgG	Immunoglobulin G
LoA	Limit of Agreement
Log	Logarithm
MNA	Microneutralization Assay
NMRC	Naval Medical Research Center
PASS	Prospective Assessment of SARS-CoV-2 Seroconversion
%	Percent
PNA	Pseudovirus Neutralization Assay
P	Probability Value
PI	Principal Investigator
PRNT	Plaque Reduction Neutralization Test
pVNT	Pseudo-based Neutralization Test
RBD	Receptor Binding Domain
ROC	Receiver Operating Characteristic
SARS-CoV-2	Severe Acute Respiratory Syndrome Coronavirus 2
S	Spike
SD	Sample Diluent
sVNT	Surrogate Virus Neutralization Test
USUHS	Uniformed Services University of Health Sciences
VNA	Virus Neutralization Assay
VOC	Variant of Concern
WT	Wild Type

INTRODUCTION

Coronavirus disease (COVID-19) is an infectious respiratory illness caused by the severe acute respiratory syndrome coronavirus 2 (SARS-CoV-2). The novel coronavirus was first discovered in 2019 in Wuhan, China and in early 2020, the World Health Organization declared SARS-CoV-2 a pandemic, currently resulting in millions of infections and fatalities. A major challenge in combating COVID-19 is to determine the immune response correlates of protection for vaccines or following natural infection. Correlates of protection are measurable parameters that indicate if an individual has protective immunity against a pathogen. Disease-specific antibodies are examples of biomarkers that are measurable immunological correlates of protection (Chen et al. 2013). Binding antibodies (BAbs) bind to pathogens but do not directly interfere with their infectivity (Coronavirus…2020). These antibodies are also known as non-neutralizing antibodies, which are important to flag foreign antigens from invading pathogens for immune cells to destroy. Neutralizing antibodies directly bind to a pathogen in a manner that blocks infection of cells (Payne 2017). While both binding and neutralizing antibodies are thought to be potential correlates of protection against COVID-19 (Feng et al. 2021), several studies recently, have connected vaccine efficacy with neutralizing antibody responses to SARS-CoV-2 (Earle et al. 2021; Khoury et al. 2021).

SARS-CoV-2 Immune Response

SARS-CoV-2 infection from vaccination or natural exposure induces a humoral immune response in a human host. The general steps (Figure 1) in human antibody response to SARS-CoV-2 infection are initiated with viral entry via the interaction

between the viral S protein and the host angiotensin-converting enzyme 2 (ACE2) (Ghaffari et al. 2020). Following viral entry, the virus replicates and releases from the host cell and a subset of viruses are ingested by antigen presenting cells (APCs) (Ghaffari et al. 2020). The APCs then present the fragmented SARS-CoV-2 antigen(s) to T helper cells, which in turn will interact and activate B cells (Ghaffari et al. 2020). Next, the activated B cells differentiate into plasma or memory B cells, where the plasma cells secrete their SARS-CoV-2-specific receptors in the form of IgM, IgG, or IgA antibodies; and antibody-mediated neutralization occurs when SARS-CoV-2-specific antibodies bind to viral antigen(s) preventing virus interaction and entry into host cells (Ghaffari et al. 2020).

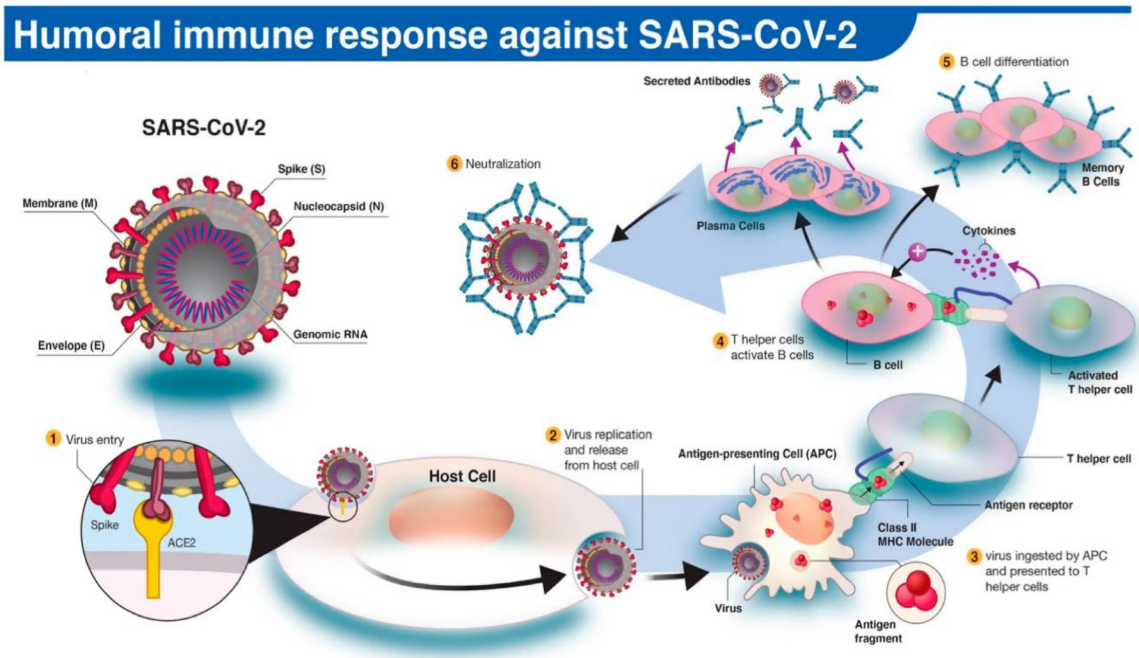

Figure 1. Schematic illustration of the humoral immune response to SARS-CoV-2 infection. General steps highlighting the main events of the human antibody response to SARS-CoV-2 infection, starting from virus entry to neutralizing antibody production (Ghaffari et al. 2020; reused under the CC BY license 4.0).

SARS-CoV-2 Virion Structure

SARS-CoV-2 belongs to the *Betacoronavirus* genus in the *Coronaviridae* family and is a positive-sense RNA virus with a viral genome that encodes four major structural proteins: membrane (M), envelope (E), nucleocapsid (N) and S (Figure 2) (Du et al. 2021; Pang et al. 2021). The S protein is a transmembrane homotrimeric class I fusion glycoprotein, composed of two subunits, S1 and S2, both in each S monomer (Sternberg and Naujokat et al. 2020; Lan et al. 2020). A subdomain in the S1 subunit, located at the apex, is the RBD that undergoes conformational movements between a transiently open/up status and a closed/down status (Sternberg and Naujokat et al. 2020).

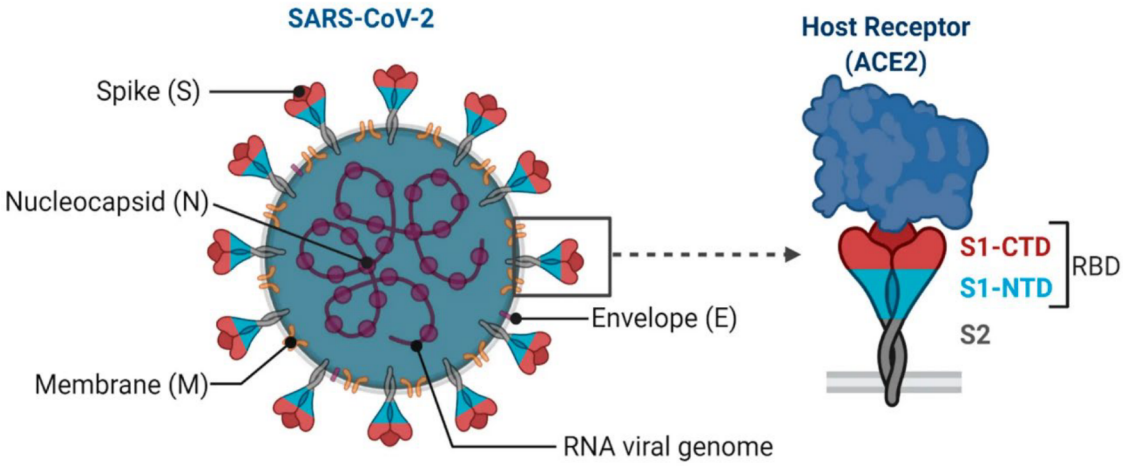

Figure 2. Schematic illustration of the SARS-CoV-2 virion structure and outbreak of S protein. SARS-CoV-2 viral genome encodes four major structural proteins, the envelope (E) protein, membrane (M) protein, nucleocapsid (N) protein and S protein. The S protein monomer contains two subunits, S1 and S2. The RBD is located at the apex of the S1 subunit. S1-RBD key role is recognizing and binding to the ACE2 host receptor to initiate SARS-CoV-2 viral entry (Jain et al. 2020; reused under the CC BY license 4.0).

To initiate SARS-CoV-2 infection, the glycosylated S proteins on the surface of the virion interacts with the host cell receptor ACE2, then undergoes conformational changes that allow protease cleavage of S allowing the S2 fusion domain to facilitate

virus entry into the cell. The human ACE2 was shown to be the main functional receptor mediating viral cell entry (Tan et al. 2020; Huang et al. 2020). The RBD within the S protein is a critical target for neutralizing antibodies. Neutralizing antibodies targeting the S protein interferes with the viral S protein RBD and ACE2 receptor interaction and prevents viral entry into host cells (Figure 3) (Du et al. 2021).

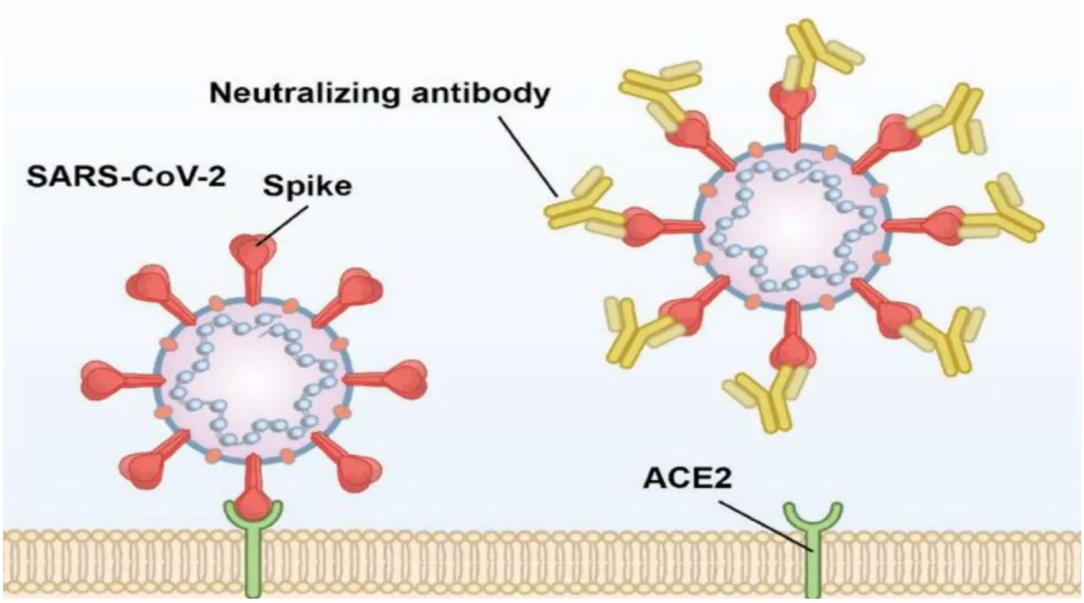

Figure 3. Schematic illustration of the SARS-CoV-2 viral entry. SARS-CoV-2 S glycoprotein RBD interaction with the ACE2 host cell receptor for SARS-CoV-2 viral entry (left). Neutralizing antibody interaction with the SARS-CoV-2 S glycoprotein RBD blocking SARS-CoV-2 viral entry (right) (Brown et al. 2021; reused under the CC BY license 4.0).

Viruses, including SARS-CoV-2, evolve as mutations occur. Some mutations affect important functional properties such as the interaction of the virus with the host cell receptor, while other mutations have little to no effect on the virus at all (Goher et al. 2021). A mutation is a single change in viruses' genetic sequence and a variant is a viral genome that may contain one or more mutation(s) (COVID-19: SARS-CoV-2… 2020). SARS-CoV-2 variants are classified as a variant of concern (VOC) when they are

associated with evidence of severe disease, an increase in transmissibility, and/or significant reduction in neutralization by antibodies. (COVID-19: SARS-CoV-2…2020). As of May 2021, the Delta (B.1.617.2) variant became a VOC. The Delta variant has mutations in the S protein that include two mutations in the RBD reported to affect virus neutralization and transmissibility (Goher et al. 2021).

Virus Neutralization Assays

Serological tests are used to determine if a person has antibodies against a specific pathogen and enzyme-linked immunosorbent assays (ELISA) are typically used to detect total BAbs (Day 2015). A virus neutralization assay (VNA) is used to determine if antibodies have neutralizing activity (Figure 4). There are different formats of VNAs that are cell-based assays and use live virus or pseudovirus to detect neutralizing antibodies. Recently, ELISA-based surrogate VNAs have been developed to detect neutralizing antibodies to SARS-CoV-2.

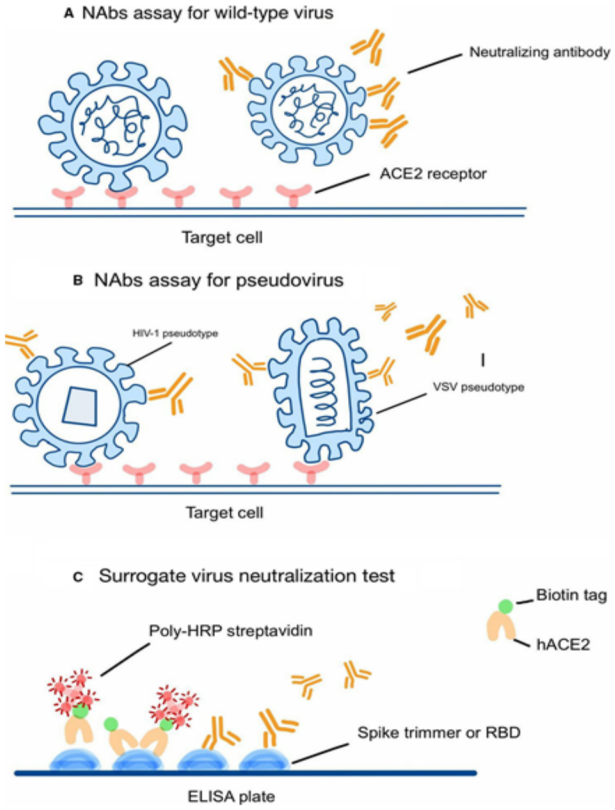

Figure 4. Schematic describing the principles of a live virus, pseudovirus and surrogate neutralization assays. A.) portrays when live SARS-CoVs-2 binds to neutralizing antibodies it inhibits the appearance of CPE and loses infectivity. B.) portrays a pseudovirus with SARS-CoVs-2 envelope. C.) portrays ELISA-based assay using recombinant ACE2 for the detection of S RBD that have not been blocked by a neutralizing antibody (Lu et al. 2021).

Cell-based neutralization assays that utilize wild type (WT) live virus are the gold standard for detecting and measuring neutralizing antibody titers. This well-established assay must be performed at the appropriate biosafety containment level. Some viruses are required to be handled in high containment (i.e. BSL-3 or BSL-4 laboratories), which makes performing these cell-based VNAs impractical for routine clinical laboratory practice. Some examples of cell-based VNAs include plaque reduction neutralization test (PRNT) and microneutralization (MN) assays. The PRNT is based on a plaque assay, which is a well-established method for determining virus concentration by counting the number of plaque forming units in a monolayer of infected cells. This assay typically

uses 6, 12, or 24-well plates and is therefore considered low-throughput, which makes it difficult to analyze large numbers of samples. In contrast, the MN assay is typically performed in 96-well plates, which increases assay throughput. MN assays visualize infected foci via immunostaining, which is then counted using computer-controlled imagers or read on an enzyme-linked immunosorbent assay (ELISA) plate reader measuring a colorimetric dye (Bewley et al. 2021).

Pseudovirus neutralization assays (PNAs) are cell-based but do not contain live virus. PNAs utilize genetically modified nonreplicating virions that comprise the enzymatic and structural core of one virus, the surface protein of another virus, and a reporter gene (Bewley et al. 2021). One approach PNAs use is pseudotyping lentiviral particles with SARS-CoV-2 S protein (Figure 5) (Crawford et al. 2020). In this method, 293T cells are co-transfected with a plasmid expressing S, a plasmid encoding a lentiviral backbone and plasmids expressing the other HIV proteins needed for virion formation (i.e. Tat, Gag-Pol, and Rev) (Crawford et al. 2020). The transfected cells produce lentiviral particles with S protein on their surface and these viral particles can infect cells that express the ACE2 receptor (Crawford et al. 2020).

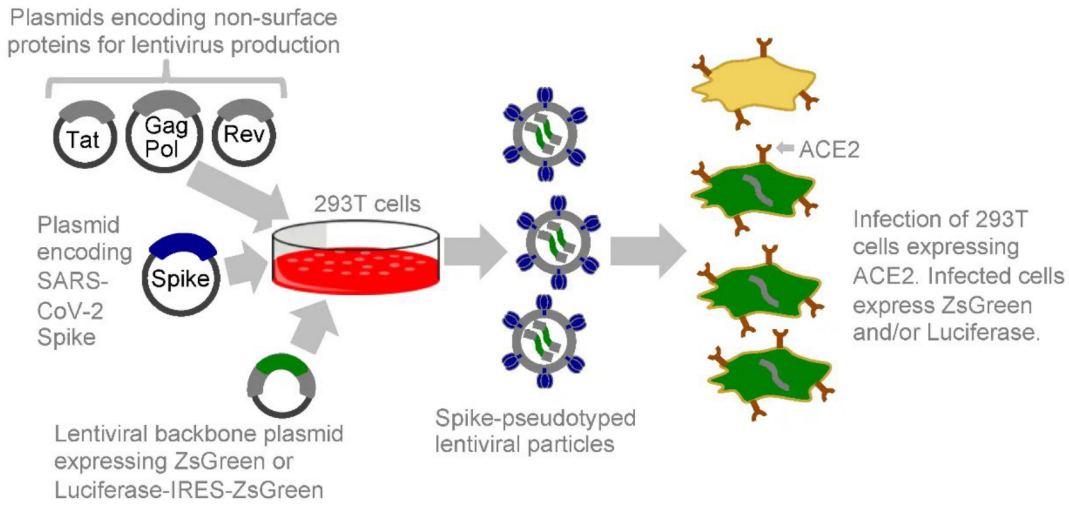

Figure 5. Basic strategy for pseudotyping lentiviral particles with SARS-CoV-2 S protein. 293T cells are co-transfected with the following: (plasmid encoding lentiviral backbone, plasmid expressing S, and plasmids expressing the HIV proteins needed for virion formation (i.e. Tat, Gag-Pol, and Rev). The transfected cells produce lentiviral particles with S protein on their surface and these viral particles can infect cells that express the ACE2 receptor (Crawford et al. 2020; reused under the CC BY license 4.0).

PNAs involve incubating the pseudovirus and cells in the presence of different antibody concentrations of interest and using an instrument to detect the reporter gene such as a plate luminometer to measure the light emission (Pseudovirus neutralization… 2021). PNAs can routinely evaluate neutralizing antibodies in a BSL-2 laboratory due to the nature of pseudoviruses being genetically stable and noninfectious (Steward 2021).

Surrogate virus neutralization assays (sVNTs) substitutes the need for live/pseudo virus and cells used in VNAs. The sVNT is designed to mimic the virus-host interaction and measures the competitive inhibition of this interaction (Tan et al. 2020 and Lou et al. 2021). The SARS-CoV-2 sVNTs are based on the principle that neutralizing antibodies bind S1-RBD and block the interaction between the RBD and the ACE2 receptor (Lu et al. 2021). Some sVNTs are ELISA-based and use reduction of horseradish peroxidase

(HRP) luminescence signal to detect the presence of antibodies that blocks the RBD-ACE2 interaction (Lu et al. 2021). sVNTs do not require live virus nor cells and can be run in BSL-2 laboratories (Lu et al. 2021). A comparison of the sVNT to the cell-based VNAs is included in Table 1.

Table 1. Comparison of cell-based and surrogate VNAs

VNAs	Mechanism	Design	Time	Safety
Plaque Reduction Neutralization Test	Live Virus/ Cell-Based	6, 12 or 24 well plate	5 days	BSL-3
Microneutralization Assay	Live Virus/ Cell-Based	96 well plate	2-4 days	BSL-3
Pseudo Neutralization Assay	i.e. HIV-Lentiviral System / Cell-Based	96 well plate	2-3 days	BSL-2
Surrogate Virus Neutralization Test	Purified Protein-Protein Interaction/ELISA-Based	96 well plate	1-3 hours	BSL-2

Abbreviations: VNAs: Virus Neutralization Assays; BSL: Biosafety level; HIV: Human immunodeficiency virus; ELISA: Enzyme-linked Immunosorbent Assay.

The emergence of the novel SARS-CoV-2 has highlighted the need to develop safer and more efficient platforms to detect and quantify neutralizing antibodies. Recently, several studies have evaluated live and pseudo VNAs in comparison to sVNTs. Tan et al. (2020) reported a SARS-CoV-2 sVNT that detected total immunodominant neutralizing antibodies targeting the S protein RBD and then conducted a comparison study using sera from COVID-19 patients and demonstrated a good correlation between the sVNT and live VNA and PNA (Tan et al. 2020). Valcourt et al. evaluated a commercially available sVNT by conducting a comprehensive comparison between the sVNT and an in-house PRNT (Valcourt et al. 2021). They reported that the sVNT in the study demonstrated similar or greater detection of neutralizing antibodies in COVID-19 specimens; however, there was a high non-neutralizing antibody detection rate for

PRNT –negative COVID-19 samples, suggesting an over-estimation of functional neutralizing antibody response (Valcourt et al. 2021). Von Rhein et al. compared a competition ELISA-based sVNT to a PRNT and PNA to determine the SARS-CoV-2 neutralizing activity and found that while the neutralization activity correlated among the different methods, the sVNT assay overestimated the samples with low neutralizing activity (von Rhein et al. 2021). The aforementioned studies and other current SARS-CoV-2 sVNTs use platforms that are operator dependent as opposed to an automated platform.

Automated Immunoassay Platform

The sVNT could be improved with more automated immunoassay technology. Protein Simple developed Simple Plex™, a novel automated immunoassay platform (Aldo et al. 2016). This integrated immunoassay system consists of the Ella instrument (microfluidic automated analyzer) and a disposable microfluidic cartridge for the assay reagents and samples (Aldo et al. 2016). There is an array of Simple Plex™ flexible cartridge options (single plex, multianalye, multiplex and customizable) that can be tailored to specific project scope and throughput (Simple Plex Assays… 2021). The Simple Plex™ customizable cartridge (Figure 6) in particular, provides additional inputs in the cartridge and uses an anti-digoxigenin (Dig) capture antibody to serve as a foundation to allow for one to flexibly build a specific immunoassay using their own reagents (Customizable assays… 2022). The Simple Plex™ microfluidic (single plex, multianalye, and multiplex) cartridges require no manual steps, washes, or reagent additions once sample and buffer are loaded (Ella… 2017). The Simple Plex™

automated platform allows samples to flow through microfluidic channels over coated triplicate glass nano reactors (GNRs) (Ella… 2017), run all the immunoassay operations and produce signal levels from each GNR, (Aldo et al. 2016) comprised of single digit coefficient of variations (CV) and minimal variability in about an hours' time (Ella… 2017).

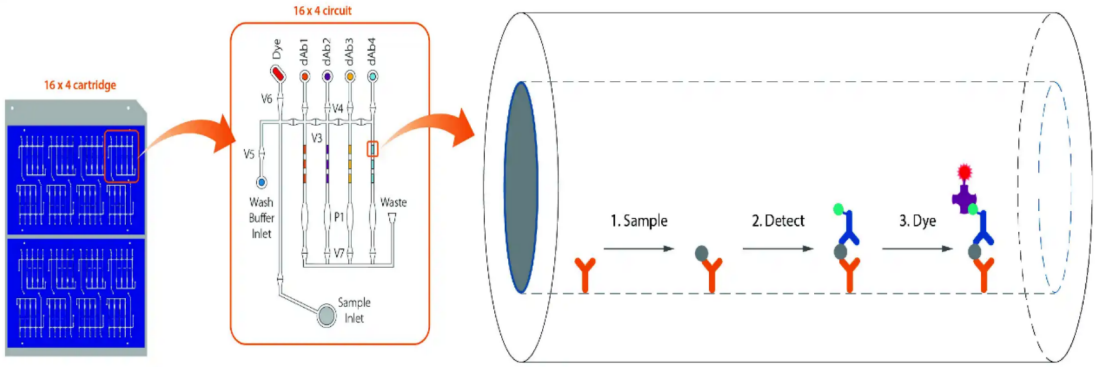

Figure 6. Backside view of the 16x4 multi-analyte Simple Plex™ cartridge (left). Each individual sample runs through a microfluidic circuit (middle) where the automated sandwich immunoassays are performed in the GNRs (right**)** (Labant 2016).

Objectives and Rationale

In this project, we hypothesized that similar titers of neutralizing antibodies can be detected using the Simple Plex™ sVNT as compared to more traditional cell-based neutralization assays. Our focus is evaluating a SARS-CoV-2 sVNT on the Simple Plex™ automated immunoassay platform that can detect and quantify neutralizing antibodies and has the ability to determine neutralizing activity of emerging variants. Our initial goal was to develop an automated sVNT and compare it to an MN and PNA using the same sample cohort. Our second goal was to evaluate the automated sVNT against the Delta-S1-RBD compared to the WT-S1-RBD. This assay was originally developed

based on the S1-RBD for the Wuhan isolate, which is at the root of the current pandemic and is considered the WT strain. A major advantage of the sVNT assay is that the recombinant S1-RBD protein can be modified quickly based on known sequence from emerging variants. Therefore, the goal of this project was to evaluate if this SARS-CoV-2 sVNT would provide a more rapid, less labor intensive, and automated approach to determine the titers of neutralizing antibodies on a larger scale compared to MN and PNA, and provide an approach to quickly evaluate the neutralizing activity of emerging variants. Our results demonstrate that the automated and rapid SARS-CoV-2 strongly correlate and had strong association with the live virus MN assay. Our results also demonstrate the feasibility of the sVNT to assess neutralizing antibody activity against future emerging SARS-CoV-2 variants.

MATERIALS AND METHODS

Serum Samples

A negative panel sourced by the BEI resources that consisted of 50 known negative serum samples that were collected prior to the emergence of SARS-CoV-2. A specificity panel sourced by the Department of Defense (DoD) serum repository consisted of a mixed panel of 50 serum samples positive for seasonal human coronaviruses (229E, HKU1, NL-63, OC-43) and influenza A/B. The negative and specificity panels were used to establish a negative cutoff value for the sVNT assay.

The Prospective Assessment of SARS-CoV-2 Seroconversion (PASS) study collected 206 serum samples from volunteer healthcare workers at Walter Reed National Military Medical Center. At the start of the PASS study, each volunteer was confirmed negative for SARS-CoV-2. From the 206 serum samples provided, 103 were pre and 103 were post-vaccination (time point: 1-month after the second dose of the Pfizer vaccine) samples. SARS-CoV-2 neutralizing antibodies were evaluated using samples that tested positive by an assay developed for the qualitative detection of human SARS-CoV-2 antibody in serum by ELISA described by Amanat et al. (2020). The patient sera samples from the PASS study were tested by other laboratories to determine neutralizing antibody titers by a MN and PNA. The same cohort of PASS serum samples were used to determine SARS-CoV-2 neutralizing antibody titers by sVNT on the Ella analyzer and the results were compared to those endpoint titers determined by the MN and PNA used for this project.

Assay Reagent Preparation

Dig labeling

Each S1-RBD was conjugated with Dig. Following a slightly modified version of the procedure outlined in the Simple Plex™ (Bio-Techne, San Jose, CA) Protein Simple Quick Start Guide, WT recombinant SARS-CoV-2 S RBD Fc Chimera (R&D Systems, Minneapolis, MN 10499-CV-100) and Delta B.1.617.2 recombinant SARS-CoV-2 S RBD Fc Chimera (R&D Systems 10901-CV-100) were Dig NHS (Enzo Life Sciences, Farmingdale, NY ENZ-45022) labeled at a protein concentration of 0.5mg/mL using a 5:1 molar ratio (Dig/Protein). The protein concentration of each RBD was determined using the Bicinchoninic acid (BCA) Protein Assay Kit -23227 (Pierce™) (Thermo Fisher Scientific Rockford, IL). The Dig conjugated S1-RBDs were then stabilized with BSA and the final concentrations were adjusted as described in the Quick Start Guide.

ACE2-Histidine (His) Half-maximal Effective Concentration (EC_{50}) Determination

The EC_{50} of the ACE2-His was determined for both S1-RBDs. ACE2-His (R&D Systems 933-ZN) was serially diluted 1:5 from 50,000ng/ml to ~.001ng/ml, a total of 12 dilution points. Using a Simple Plex™ 48-Dig cartridge and a layout suggested by Protein Simple, ACE2-His binding to the Dig-S1-RBDs (WT and Delta) was assessed by reacting the ACE2-His dilution series with 10 ug/mL each of the two Dig-S1-RBDs in duplicate. The Dig-S1-RBDs were added to the capture inlets and the ACE2-His dilution points to the sample inlets. Biotin anti-His was added to the detector inlets. The relative fluorescence unit (RFU) means generated from the Ella analyzer were used to calculate the respective ACE2-His half maximal effective concentration (EC_{50}) values for each S1-RBD recommended by Protein Simple. The model used to calculate the EC_{50} in

GraphPad Prism is further described in the statistical analysis section. The WT ACE2-His EC_{50} value is 4.959e -009 and the Delta ACE2-His EC_{50} value is 4.784e -009. The ACE2 concentration based on the calculated EC_{50} values (10nM for WT and 5nM for Delta) were used for the sVNT assay. See (Figure 7) for respective ACE2-His EC_{50} values.

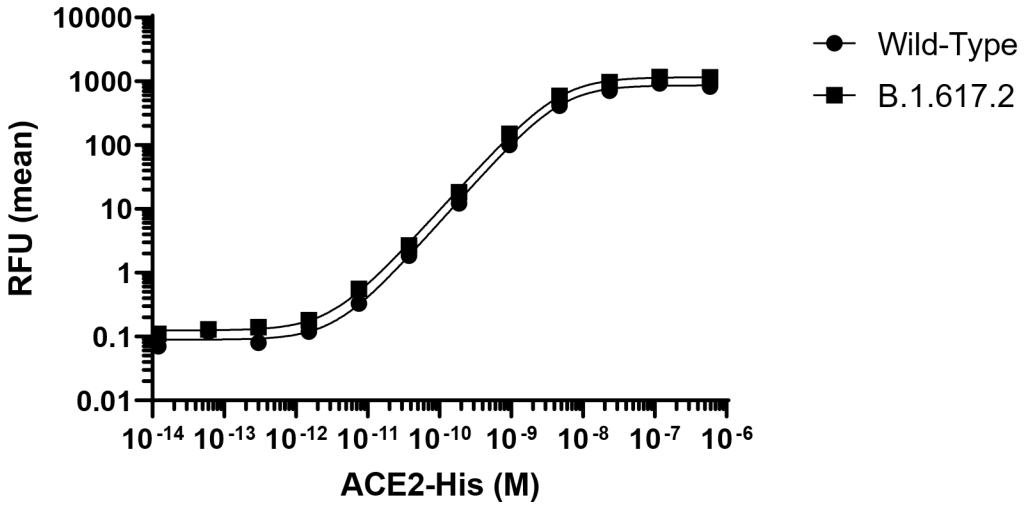

	Wild-Type	B.1.617.2
EC_{50}	4.959e- 009	4.784e- 009

Figure 7. The ACE2-His half-maximal effective concentration (EC_{50}) values for the WT and Delta variant S1-RBDs. The EC_{50} values were recommended by Protein Simple to determine the final ACE2-His concentrations for the WT-sVNT and Delta-sVNT (Copyright 2022 ProteinSimple Corporation, reprinted/adapted with permission).

Automated sVNT

The customizable open cartridge (Figure 8) was chosen to design the sVNT assay, this allowed for the utilization of the anti-dig capture antibody feature and flexibility of initial capture and detector reagent addition.

The Dig-labeled S1-RBD (WT/Delta) capture antigens were prepared at 10ug/mL in provided sample diluent (SD) 13 and the biotinylated mouse anti-His tag (R&D Systems BAM050) detector was prepared at 3.33 ug/mL in SD13 diluent. In a polypropylene sample prep plate, sera samples were diluted 1:5 (2X) in 1X SD19 diluent. The ACE2-His was prepared for the WT S1-RBD at 2×10^{-8} and prepared at 1×10^{-8} for the Delta variant S1-RBD, based on the calculated EC_{50} values. The human COVID S Protein monoclonal antibody CR3022 (WRAIR EG 03-13-20) was diluted in normal human sera to 30ug/mL and 0.3ug/mL to serve as the high and low respectively positive controls and 30ul of 1X SD19 to serve as the negative control.

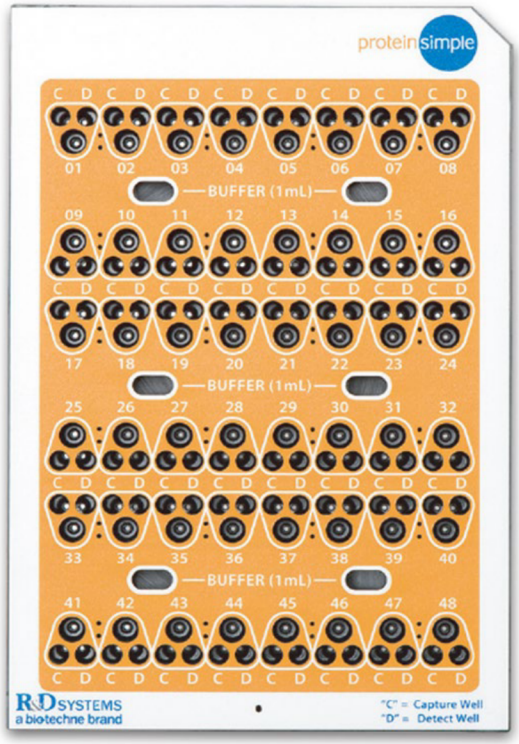

Figure 8. Image of the (front side) customizable 48-Dig open Simple Plex™ cartridge (R&D Systems) developed by Protein Simple. Each inlet has a capture (C) input, detector (D) input, and a sample input. There are 6 inputs in between rows to place the wash buffer. (Customizable assays… 2022) (Copyright 2022 ProteinSimple Corporation, reprinted/adapted with permission).

Assay Design

The Ella-based SARS-CoV-2 sVNT used in this study employs the Simple Plex™ 48-Dig customizable open cartridge. Each of the 48 inlets is an assay cluster (sample, capture and detector ports) containing triplicate GNRs functionalized with an anti-Dig antibody. Dig labeled WT and Delta S1-RBDs were used as capture antigens in alternating rows. Serum samples (3 per assay) were serially diluted 1:3 from an initial 1:10 dilution (7 points total) in a sample mixing plate. ACE2-His was prepared at two concentrations based on the EC_{50} values determined for the WT and Delta S1-RBDs. The sample dilution series were each split into two assigned rows in the sample mixing plate

followed by combination with an equal volume of ACE2-His; one row each for the two ACE2-His concentrations (i.e. WT and Delta). Each ACE2- His was also combined with the WT/Delta blanks and the high and low controls. Dig labeled S1-RBD capture antigens and the biotinylated mouse anti-His tag detector antibody were pipetted into the appropriate cartridge inlets. The sample dilution points combined with ACE2-His were then transferred from the sample processing plate rows to the corresponding rows (sample inlet ports) of the cartridge illustrated in Figure 9. The negative panel followed the (1:3 dilution in 1X SD19) (7 points total) like the pre/post samples, however, the specificity panel (HCoVs/influenza A/B sample sets) were serially diluted (1:3 in 1X SD19); a total of 3 dilution points, allowing for 6 separate samples to be analyzed on the same cartridge.

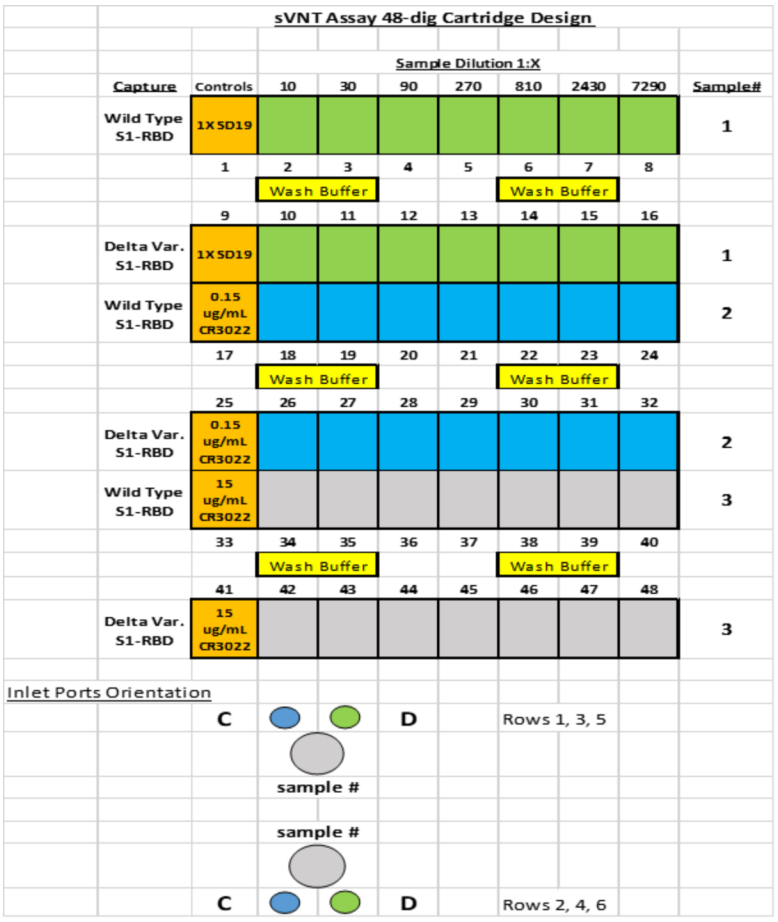

Figure 9. The 48-dig customizable open cartridge sVNT vertical design layout. The open cartridge consists of 48 inlets: each inlet comprised of a capture, detector and sample inlet port and six wash buffer inlet ports.

Following the immunoassay sandwich, when a patient sera sample contained a low neutralizing antibody titer, ACE2-His outcompeted the antibodies for the immobilized S1-RBD and thus generated a high signal as a result of binding with the biotin anti-His detector antibody and subsequent interaction with the streptavidin fluorophore (Figure 10 [left]). Conversely, when a patient sera sample had a high neutralizing antibody titer, the serum antibodies outcompeted the ACE2-His for the S1-RBD and a low signal resulted (Figure 10 [right]).

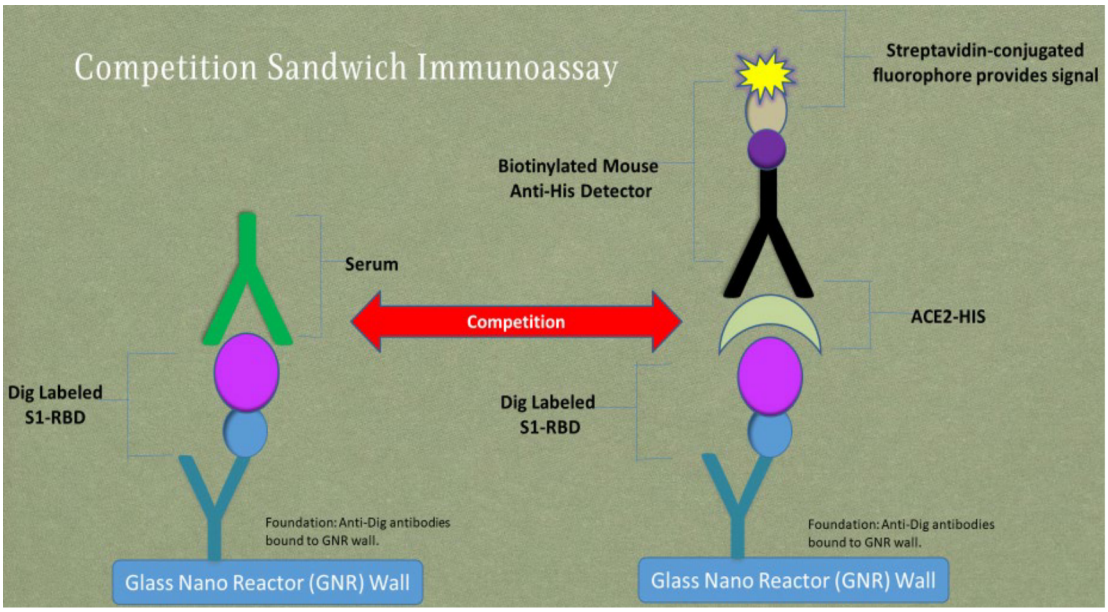

Figure 10. Schematic illustration of the competition sandwich immunoassay. The post-vaccination sera samples (right) competing with the ACE2-His (left) to bind to the S1-RBDs immunoassay competition design by Protein Simple used in the sVNTs.

.

Following addition of sera and detecting reagents, the cartridge was centrifuged at 50 x g for 15 seconds, and loaded into the Ella instrument for analysis. Assay results were obtained in 77 minutes. Average RFU values were generated for each sample. Individual RFU values for each of the triplicate GNRs were also presented. The criteria was set for sample repeat when the %CV from the triplicate RFU values per inlet were greater than 10%, all negative and high controls outside of 3 standard deviations of one another and/or no GNRs were detected.

Calculations/Statistics

% Inhibition Calculation

Each RFU mean generated from the Ella analyzer was converted into a % inhibition value. The % inhibition for each sample at every dilution point was calculated using the following formula: Inhibition [%] = (1 – (RFU mean/ Negative Control)) x 100.

The negative % inhibition values were changed to zero % inhibition for graphing purposes.

Statistical Analysis

Receiver Operating Characteristic (ROC) analyses was used to determine specificity and sensitivity for the sVNT negative cutoff. Half maximal inhibitory concentration (IC_{50}) neutralizing antibody titer values were initially calculated from the % inhibition values for each sample dilution point using the nonlinear regression curve fit analysis: [Inhibitor] vs. response - Variable slope (four parameters) model, IC_{50} values calculated the same as the EC_{50}, then agreed to use EC_{50} for nomenclature ease. The 80% of maximal effective concentration (EC_{80}) was calculated from the % inhibition values for each sample dilution point using the nonlinear regression curve fit analysis: [Agonist] vs. response – Find ECanything model. Any EC_{50}/EC_{80} calculation that was labeled as ambiguous was identified as an outlier in analysis. Prior to any correlation and hypothesis testing, all of the sample sets' EC_{50}/EC_{80} neutralizing antibody titers were logarithm $(log)_{10}$-transformed after lognormal distribution was recommended in the normality and lognormality analyses. EC_{50}/EC_{80} neutralizing antibody titers were evaluated by Dunn's multiple comparison test where statistical significance was defined as $P < 0.05$.

For correlation analysis, if all of the sample sets passed the D'Agnostino and Pearson test under the tests for lognormal distribution then correlations were investigated using Pearson's Correlation Coefficient. If even just one of the sample sets did not pass the D'Agnostino and Pearson test than Spearman's rank Correlation Coefficient was used for correlation analysis Agreement between VNA methods were assessed using bias

result from Bland-Altman analysis. All statistical analyses were performed in GraphPad Prism 8.3.1.

RESULTS

In this study, serum samples were analyzed from volunteer healthcare workers before and one month after vaccination following the second dose of the BNT162b2 (Pfizer) vaccine. The samples were a part of the PASS study, which is an observational longitudinal cohort study that is evaluating the immunological responses to SARS-CoV-2 infection and vaccination of healthcare workers (Coggins et al. 2021). In part of the study, antibody testing, of immunoglobulin G (IgG) was measured and the authors found similar endpoint dilution titers of levels of spike (S)- specific IgG antibodies, receptor binding domain (RBD)-specific IgG antibodies and neutralizing antibodies (Coggins et al. 2021). Here we developed a SARS-CoV-2 sVNT on a rapid and automated immunoassay platform to detect and determine levels of neutralizing antibodies using the PASS study samples. We compared our results to those obtained by the more traditional cell-based MN and PNA.

Assay Design and Primary Data Generation

WT-sVNT is described as all sample sets tested against the purified SARS-CoV-2 WT S1-RBD capture antigen in the immunoassay design. Delta-sVNT is described as all sample sets tested against the purified SARS-CoV-2 Delta S1-RBD capture antigen in the immunoassay design. The assay design allowed for three serum samples to be analyzed, each against both the WT and Delta-S1-RBDs on the same cartridge. At the completion of each analysis, the number of GNR's detected, RFU mean values and RFU %CVs per inlet were generated by the Ella analyzer. Our pre-determined valid assay run repeat criteria were met for each sample. Table 2 contains representative results from a post-

vaccination sample at each 1:3 dilution point; against the WT/Delta S1-RBDs. For each inlet, the number of GNRs read, the mean RFU and RFU %CV are reported.

Table 2. Representative results of typical data generated by the Ella analyzer.

Post-Vaccination Sample	S1-RBD	Dilution Series [1:3]	Inlet	GNRs	Mean RFU	RFU %CV
Negative Control	Wild		1	3	516	2.87
P126-S00-1103	Wild	10	2	3	16.2	5.02
P126-S00-1103	Wild	30	3	3	61.8	3.88
P126-S00-1103	Wild	90	4	3	178	3.33
P126-S00-1103	Wild	270	5	3	347	5.2
P126-S00-1103	Wild	810	6	3	460	6.04
P126-S00-1103	Wild	2430	7	3	496	2.88
P126-S00-1103	Wild	7290	8	3	507	4.9
Negative Control	Delta		9	3	553	2.89
P126-S00-1103	Delta	10	10	3	20.7	2.88
P126-S00-1103	Delta	30	11	3	75.9	2.41
P126-S00-1103	Delta	90	12	3	219	7.18
P126-S00-1103	Delta	270	13	3	392	3.1
P126-S00-1103	Delta	810	14	3	492	3.63
P126-S00-1103	Delta	2430	15	3	522	0.62
P126-S00-1103	Delta	7290	16	3	557	1.19

Abbreviations: RBD: Receptor binding domain; GNR: Glass nano reactor; RFU: Relative fluorescence unit; CV: Coefficient of variation.

Determining the Sensitivity and Specificity

To determine sensitivity for our sVNT we tested the negative panel, pre-vaccination cohort and specificity panel against the WT and Delta S1-RBD's (Figure 11). After testing the control panel of known negative sera (collected prior to the outbreak of SARS-CoV-2), we observed the inhibition of SARS-CoV-2 RBD- hACE2 binding was below ~30% inhibition, indicating the absence of neutralizing antibodies. The inhibition of SARS-CoV-2 RBD-hACE2-His by sera from vaccinated subjects in both the WT-

sVNT and Delta-sVNT were both above 80% inhibition indicating the presence of neutralizing antibodies.

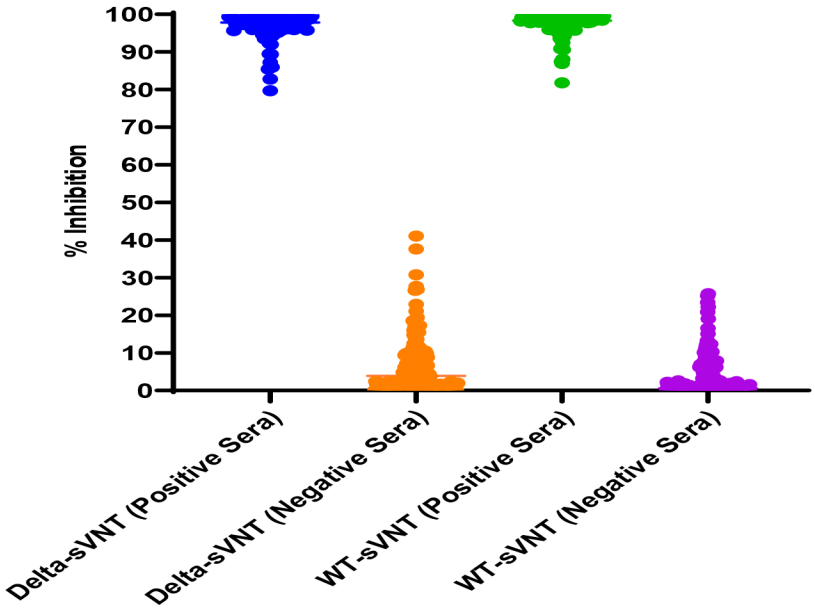

Figure 11. The % inhibition values (1:10 dilution) of the WT/Delta-sVNT to determine sVNT sensitivity. Positive sera: post-vaccination samples and negative sera: pre-vaccination samples, negative panel, and specificity panel.

To determine specificity, we tested different panels and confirmed that SARS-CoV-2 sVNT can differentiate antibody responses from those of other HCoV infections and influenza A/B. HCoVs: 229E (n=9), HKU1 (n=9), NL63 (n=10), OC43 (n=8), influenza A (n=6) and influenza B (n=8) were tested (Figure 12). These panels were tested against the SARS-CoV-2 WT/Delta S1-RBDs to demonstrate specificity and potential for cross reactivity.

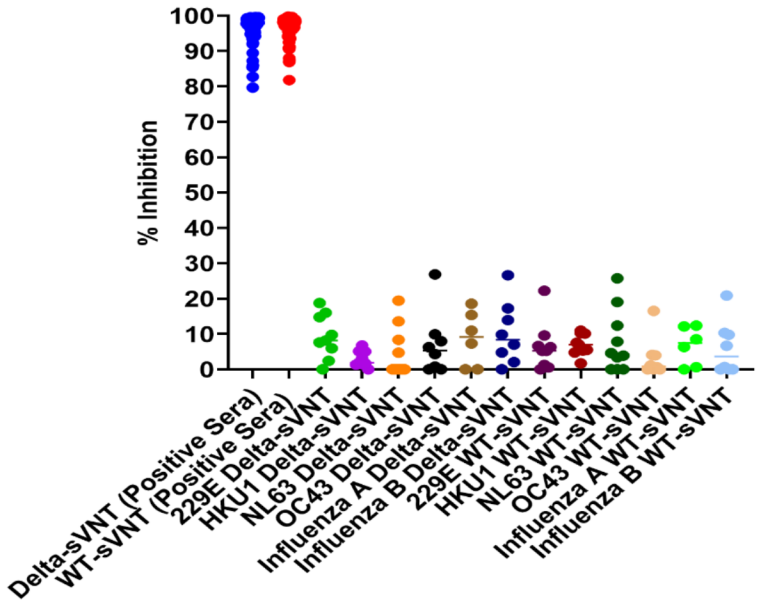

Figure 12. The % inhibition values (1:10 dilution) of the WT/Delta-sVNT to determine sVNT specificity. Post-vaccination positive samples (n=103) and HCoVs/influenza A/B samples (n=50).

Assay performance was analyzed by ROC analyses (Supplementary Table 1 and Supplementary Table 2) for the primary sensitivity and specificity cutoffs for the WT-sVNT and Delta-sVNT). ROC analysis of the WT-sVNT and Delta-sVNT each consisted of 103 positive (post-vaccination) sera samples vs a negative serum panel (specificity panel) that consisted of 103 pre-vaccination samples, 50 negative sera samples collected pre-2019, and 50 HCoVs positive or influenza A/B positive sera samples. The ROC analysis generated a cutoff of 30% inhibition using the ROC Youden J statistic, which results in a sensitivity of 100% and specificity of 100% for WT-sVNT and a sensitivity of 100% and specificity of 99% for Delta-sVNT with an area under the curve (AUC) =1.000 for both (Figure 13).

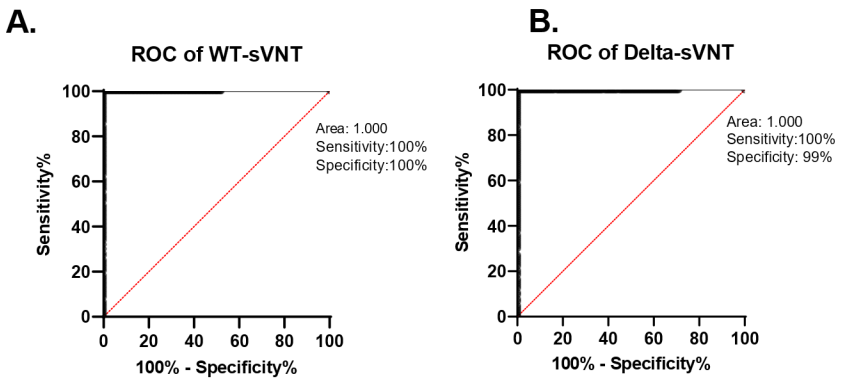

Figure 13. Determination of sVNT negative cutoff by ROC AUC/sensitivity and specificity analysis. Robustness of the sVNT assay to detect SARS-CoV-2 neutralizing antibodies. The sera tested were analyzed by ROC for A.) WT and B.) Delta.

The cutoff made the determination that any sample above 30% inhibition in the SAR-CoV-2 -sVNT was a true positive sample containing neutralizing antibodies (100% of the post- vaccination samples in the WT/Delta-sVNTs). Our established sVNT cutoff has the same inhibition cutoff as a commercially available surrogate Tan et al. (2020). All of the known positive HCoVs/influenza A/B sera samples were under the sVNT established 30% inhibition cutoff (Figure 14), which demonstrates the sVNTs ability to differentiate neutralizing antibody responses to SARS-CoV-2 compared to other respiratory viruses including the closely related HCoVs. The lower specificity of the Delta-sVNT was most likely due to three samples from the pre-vaccination sample set that were above the established 30% cutoff. A possible explanation for the lower specificity could be that prior to the study, the ELISA initially used to screen the volunteer's sera had a lower sensitivity and specificity, and some samples that were deemed negative could have had a low level of SARS-CoV-2 antibodies.

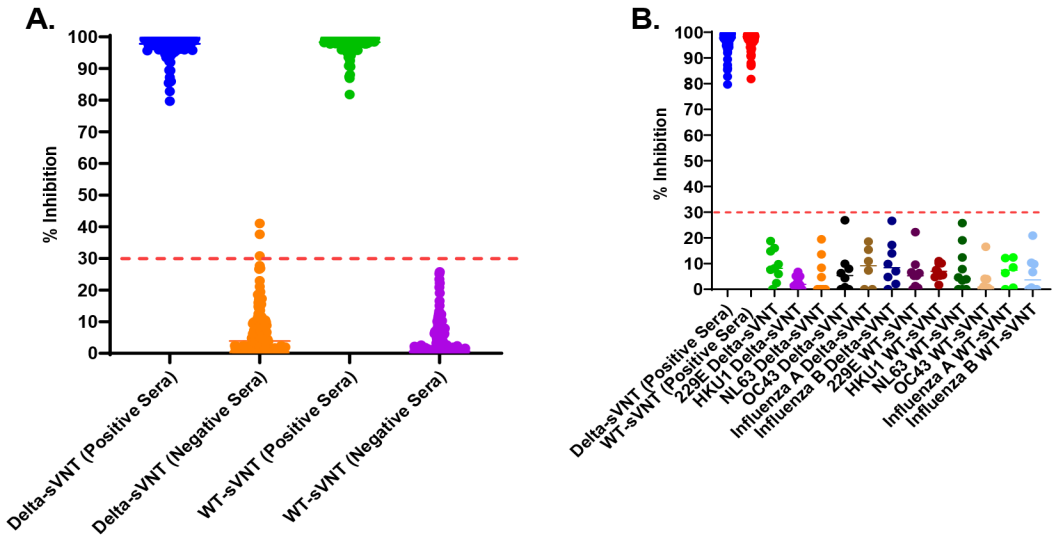

Figure 14. Established 30% inhibition sVNT negative cutoff by ROC AUC/sensitivity and specificity analysis. 30% cutoff displayed against the % inhibition values (1:10 dilution) of the WT/Delta-sVNT A.) post-vaccination positive samples, pre-vaccination samples, negative panel, specificity panel and B.) post-vaccination samples and HCoVs/influenza A/B samples.

The % inhibition curves of representative samples analyzed by the WT-sVNT and Delta-sVNT are shown in Figure 15. For all the post-vaccination samples, the inhibition decreased with sera dilution, indicating its dose-dependence. All pre-vaccination samples were below the established 30% inhibition cutoff for distinguishing positive versus negative samples. The WT-sVNT and the Delta-sVNT (pre and post-vaccination samples) displayed similar % inhibition curves. Collectively, our results demonstrate that the SARS-CoV-2 sVNT was able to effectively detect neutralizing antibodies against the respective S1-RBDs in the 1- month post-vaccination samples.

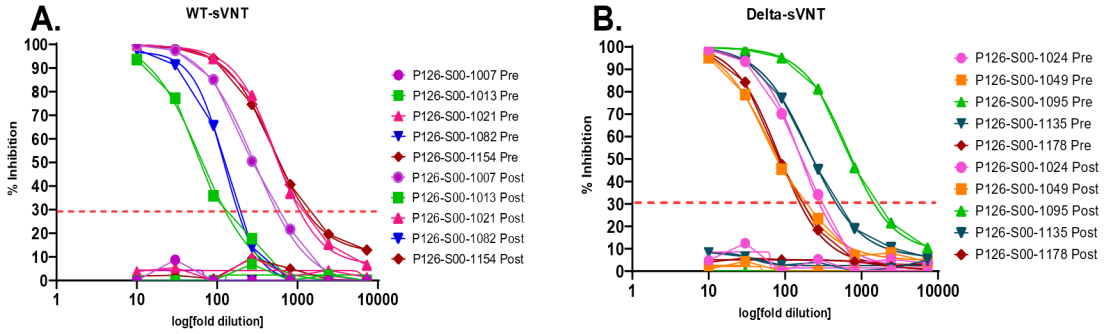

Figure 15. Inhibition of SARS-CoV-2 WT or Delta RBD-hACE2 interaction by sera representative of the (103) pre and post-vaccination samples. A.) WT-sVNT representative of the same pre and post (n=5) vaccination samples. B.) Delta-sVNT representative of the same pre and post (n=5) vaccination samples. The dotted line represents the 30% inhibition negative cutoff for distinguishing positive vs. negative samples.

EC_{50}/EC_{80} Determination and Neutralizing Antibody Comparison Analyses

The WT-sVNT and Delta-sVNT neutralizing antibody titers for each sample were determined by calculating the EC_{50} and EC_{80} titers (Supplementary Table 3 and Supplementary Table 4) from the % inhibition curves. Dr. Ed Mitre from Uniformed Services University of Health Sciences (USUHS) and the principal investigator (PI) of the PASS study provided the samples used to compare the neutralizing antibody titers between the different VNAs (Supplementary Table 5). Dr. Kevin Schully's Lab at the Naval Medical Research Center (NMRC) completed the MN on the 103 post-vaccination samples and reported the WT EC_{50} neutralizing antibody titers. Dr. Carol Weiss's Lab at the Food and Drug Administration (FDA) completed the PNA on 36 post- vaccination samples and reported WT/Delta EC_{50} neutralizing antibody titers. In this current study, we completed the sVNT on the 103-pre vaccination samples and 103-post-vaccination samples and determined the WT/Delta EC_{50}/EC_{80} neutralizing antibody titers. A cohort of 36 WT EC_{50} neutralizing antibody titers were compared across all the VNAs.

The EC_{50} neutralizing antibody titers for the cell-based assays were compared to the sVNT results for the same cohort of 1-month post-vaccination samples (n=36; Figure 16). A Dunn's multiple comparison test was performed to analyze differences in the EC_{50} neutralizing antibody titers determined by the various assays. The titers determined by the gold standard MN assay were not significantly different compared to the WT-SVNT and Delta-sVNT titers (Table 3). In contrast, we did see significant differences in the EC_{50} titers determined by the PNA when compared to the titers determined by the sVNTs. There was also a significant difference in the EC_{50} titers determined by MN compared to the PNA (Table 3).

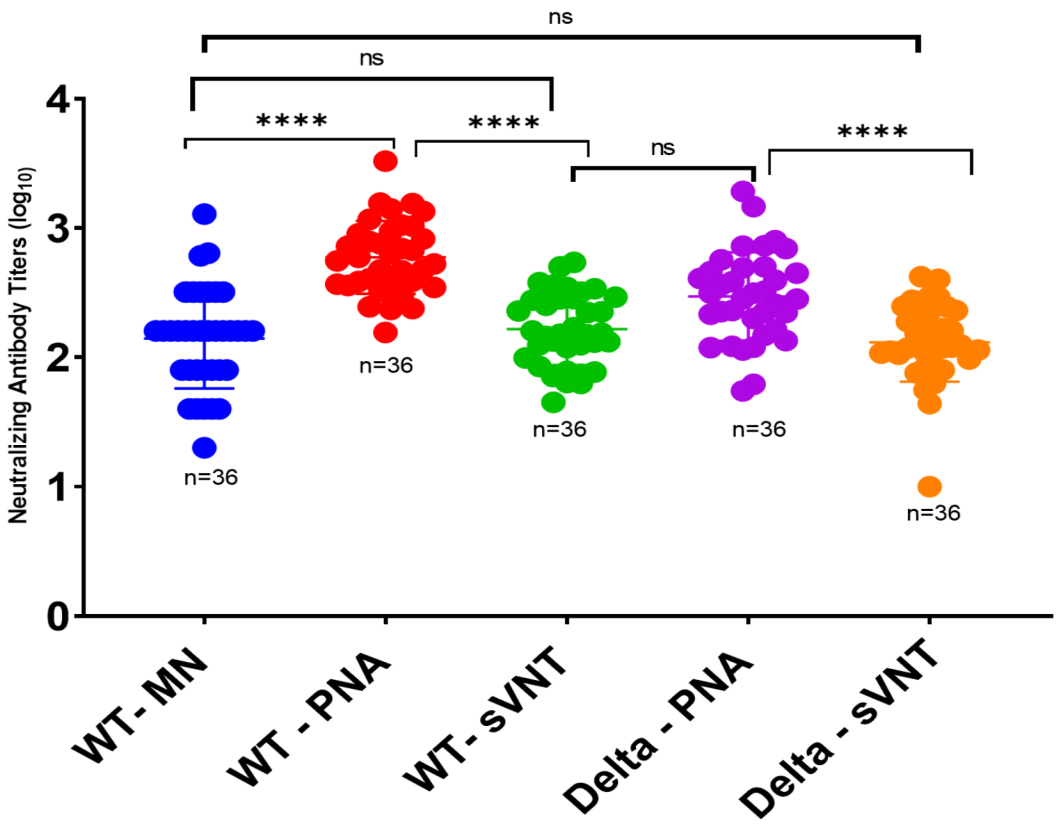

Figure 16. The EC_{50} neutralizing antibody titers determined by MN, PNA, and sVNT. The symbols represent the individual serum samples (n=36/assay), the bar represents the mean and the error bars represent the standard deviation and ns = not significant. The p-values are in Table 3.

Table 3. Dunn's multiple comparisons test results of the EC_{50} (n=36) neutralizing antibody titers of the MN, PNA, and sVNT

Dunn's multiple comparisons test	Rank sum diff.	Significant?	Summary	Adjusted P Value
WT- MN vs. WT - PNA	-96	Yes	****	<0.0001
WT- MN vs. WT- sVNT	-18	No	ns	>0.9999
WT- MN vs. Delta - PNA	-57	Yes	***	0.0002
WT- MN vs. Delta - sVNT	16	No	ns	>0.9999
WT - PNA vs. WT- sVNT	78	Yes	****	<0.0001
WT - PNA vs. Delta - PNA	39	Yes	*	0.0365
WT - PNA vs. Delta - sVNT	112	Yes	****	<0.0001
WT- sVNT vs. Delta - PNA	-39	Yes	*	0.0365
WT- sVNT vs. Delta - sVNT	34	No	ns	0.1127
Delta - PNA vs. Delta - sVNT	73	Yes	****	<0.0001

Abbreviations: EC_{50}: Half-maximal effective concentration; MN: microneutralization assay; PNA: pseudovirus neutralization assay; sVNT: surrogate virus neutraliztion test; WT-MN: Wild Type Microneutralization assay; WT-PNA: Wild Type pseudovirus neutralization assay; Delta-PNA: Delta- pseudovirus neutralization assay WT-sVNT: Wild Type surrogate virus neutralization test; Delta-sVNT: Delta-surrogate virus neutralization assay; Diff: difference; P: probability; NS: not signficant.

The EC_{50} neutralizing antibody titers for the cell-based assay MN were compared to the sVNT results for the same cohort of 1- month post-vaccination samples (n=102; Figure 17). A Dunn's multiple comparison test was performed to analyze differences in the EC_{50} neutralizing antibody titers determined by the different assays. The titers determined by the gold standard MN assay were significantly different compared to the WT-sVNT and Delta-sVNT titers (Table 4). The significant difference between the 102 samples vs the 36 samples WT-MN and WT/Delta-sVNT comparison results could be due to a difference in the sample size used for the analysis. PNA was not compared here because results were only available for 36 samples and not all 102 samples (Table 4).

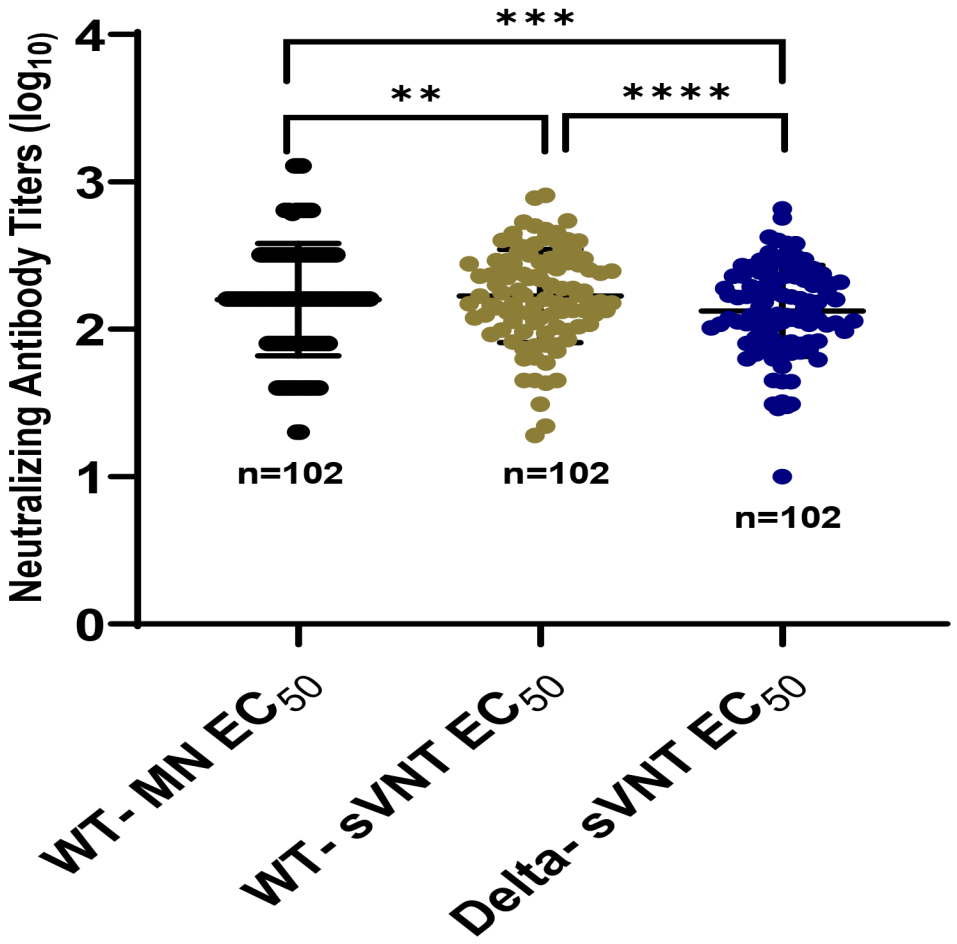

Figure 17. The EC_{50} neutralizing antibody titers determined by MN and sVNT. The symbols represent the individual serum samples (n=102/assay), the bar represents the mean and the error bars represent the standard deviation. The p-values are in Table 4.

Table 4. Dunn's multiple comparisons test results of the EC_{50} (n=102) neutralizing antibody titers of the MN and sVNT

Dunn's multiple comparisons test	Rank sum diff.	Significant?	Summary	Adjusted P Value
WT- MN vs. WT - sVNT	-43	Yes	**	0.0088
WT- MN vs. Delta- sVNT	-55	Yes	***	0.0004
WT-sVNT vs. Delta - sVNT	-97	Yes	****	<0.0001

Abbreviations: EC_{50}: Half-maximal effective concentration; MN: microneutralization assay; sVNT: surrogate virus neutraliztion test; WT-MN: Wild Type Microneutralization assay; WT-sVNT: Wild Type surrogate virus neutralization test; Delta-sVNT: Delta-surrogate virus neutralization assay; Diff: difference; P: probability.

The EC_{80} neutralizing antibody titers for the WT-sVNT were compared to the Delta-sVNT results for the same cohort of 1-month post-vaccination samples (n=102; Figure 18). A Wilcoxon matched-pairs signed rank test was performed to analyze the EC_{80} neutralizing antibody titers determined by the two assays. The EC_{80} titer medians determined by the WT-sVNT were significantly different compared to the Delta-sVNT (Table 5). These results are similar to the WT/Delta 102 sample EC_{50} significant difference in neutralizing antibody means.

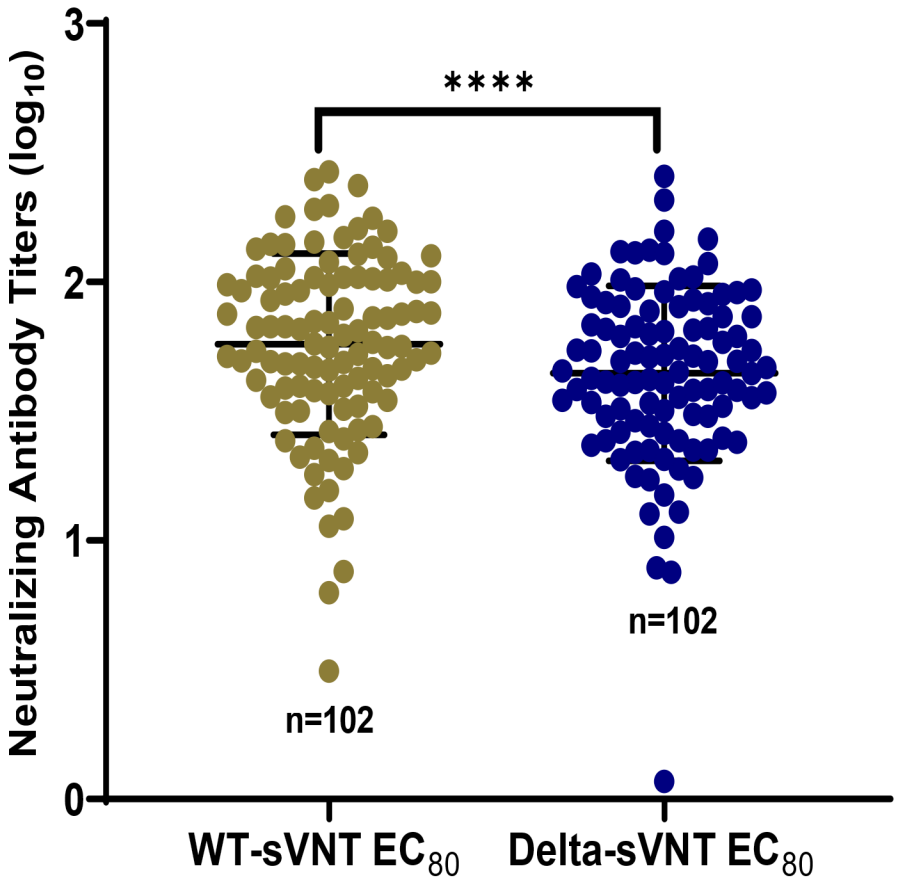

Figure 18. The EC_{80} neutralizing antibody titers determined by WT-sVNT and Delta-sVNT. The symbols represent the individual serum samples (n=102/assay), the bar represents the mean and the error bars represent the standard deviation. The p-values are in Table 5.

Table 5. Wilcoxon matched-pairs signed rank test results of the EC_{80} (n=102) neutralizing antibody titers of the WT-sVNT and Delta-sVNT

Wilcoxon matched-pairs signed rank test	Sum of signed ranks (W)	Significant?	Summary	Exact P Value
WT- sVNT vs. Delta - sVNT	-4195	Yes	****	<0.0001

Abbreviations: EC_{80}: 80% of maximal effective concentration; WT-sVNT: Wild Type surrogate virus neutralization test; Delta-sVNT: Delta-surrogate virus neutralization assay; P: probability.

A correlation analysis was used to compare the EC_{50} neutralizing antibody titers determined by MN, PNA, and the sVNT. The Pearson's correlation coefficient and simple linear regression analysis was performed for all three assays using the same cohort of 1- month post-vaccination samples (n=36; Figure 19A-C). The EC_{50} neutralizing antibody titers determined by WT-sVNT and WT-MN showed a strong positive correlation (Pearson r = 0.7203; p-value <0.0001; 95% CI: 0.5132 to 0.8481; r squared= 0.5188). Similarly, the EC_{50} neutralizing antibody titers determined by the WT-sVNT and WT-PNA demonstrate a very strong positive correlation (Pearson r = 0.8149; p-value <0.0001; 95% CI: 0.6642 to 0.9020; r squared= 0.6641). The EC_{50} neutralizing antibody titers determined by the WT-PNA and WT-MN showed a moderate positive correlation (Pearson r = 0.6158; p-value <0.0001; 95% CI: 0.3601 to 0.7854; r squared= 0.3792). Figure 19D depicts the correlation heat map between the WT-sVNT, WT-MN and WT-PNA. The statistical measure (Pearson r values), from the darkest shade (strongest) to lightest shade (weakest) are displaying the strength of the positive correlation of each the sample set comparisons. A summary of all the VNA correlation comparisons are shown in Table 6. The WT-sVNT and the WT-PNA had the strongest correlation while the WT-

PNA and WT-MN had the weakest correlation among all VNA. Overall, all the VNA comparisons have a moderate to strong positive correlation, which has similar findings with commercial sVNT studies reported by Tan et al. (2020) and Valcourt et al. (2021).

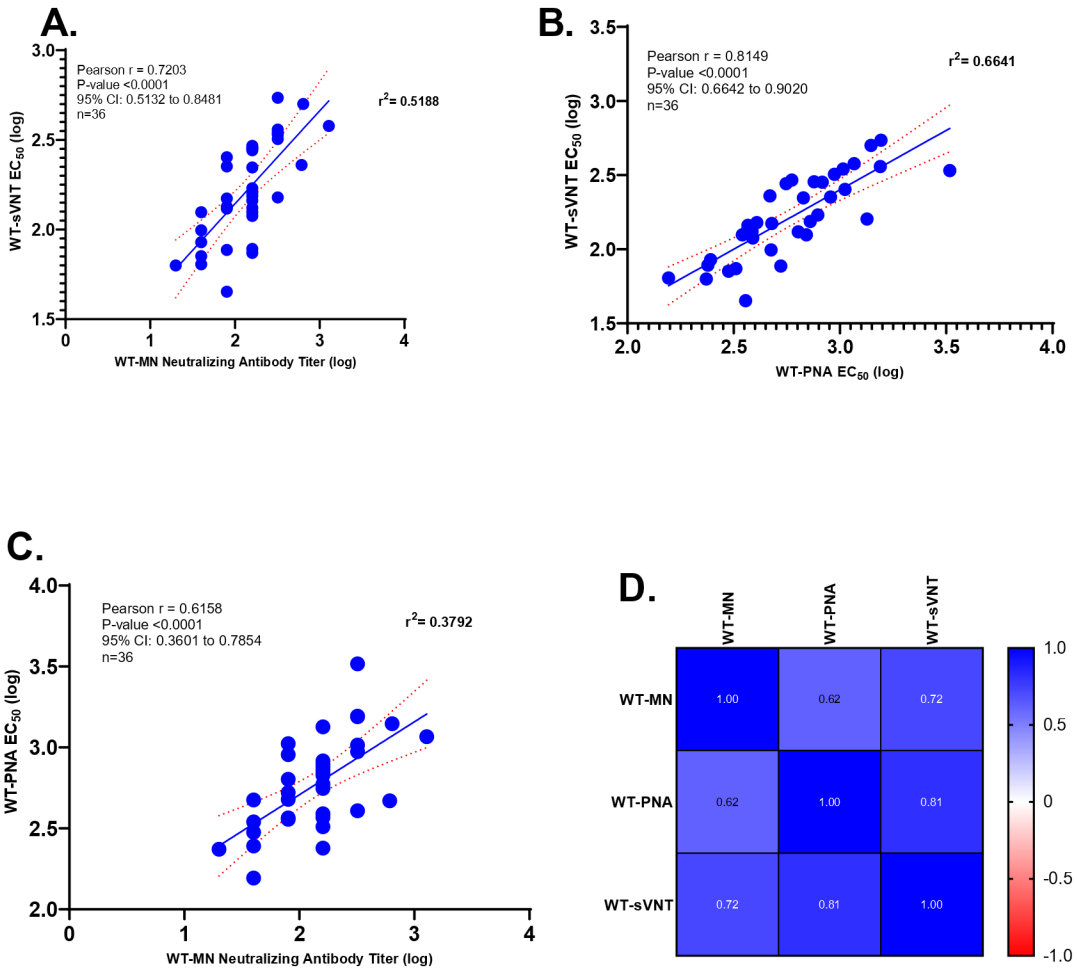

Figure 19. Correlation analysis results of WT-sVNT, WT-MN and WT-PNA to detect neutralizing antibodies against the SARS-CoV-2 WT S1-RBD. A-C) Pearson r, r squared, p-value, linear regression line (solid line), and 95% CI (dashed line), D.) Correlation heat map of post-vaccination sample panel, WT-MN (n=36), WT-PNA (n=36) and WT-sVNT (n=36).

Table 6. Correlation analysis comparison of VNAs

VNA Comparison		Pearson's r	95% CI	p-Value
WT-sVNT	WT-MN	0.7203	0.5132 to 0.8481	<0.0001
WT-sVNT	WT-PNA	0.8149	0.6642 to 0.9020	<0.0001
WT-PNA	WT-MN	0.6158	0.3601 to 0.7854	<0.0001

Abbreviations: VNA: Virus neutralization assay; WT-MN: Wild Type Microneutralization assay; WT-PNA: Wild Type pseudovirus neutralization assay; WT-sVNT: Wild Type surrogate virus neutralization test; CI: Confidence Interval; P: probability.

Additional Analysis

The EC_{50} means for the 1- month post-vaccination samples of the WT-sVNT and Delta-sVNT are displayed in Figure 20A. The mean of the EC_{50} values for WT-sVNT (2.23) and the Delta-sVNT mean (2.12) were very similar. A correlation analysis was used to compare the EC_{50} neutralizing antibody titers determined by the WT-sVNT and Delta-sVNT. The Spearman's rho and simple linear regression analysis was performed for the WT-sVNT (n=102) vs the Delta-sVNT (n=102; Figure 20B). The EC_{50} neutralizing antibody titers determined by the WT-sVNT and Delta-sVNT showed a very strong positive correlation (Spearman's rho = 0.9523; p-value <0.0001 and 95% CI: 0.9293 to 0.9680). These results suggest that the Pfizer vaccine induces a neutralizing antibody response that reacts similarly to the WT and Delta SARS-CoV-2 variants.

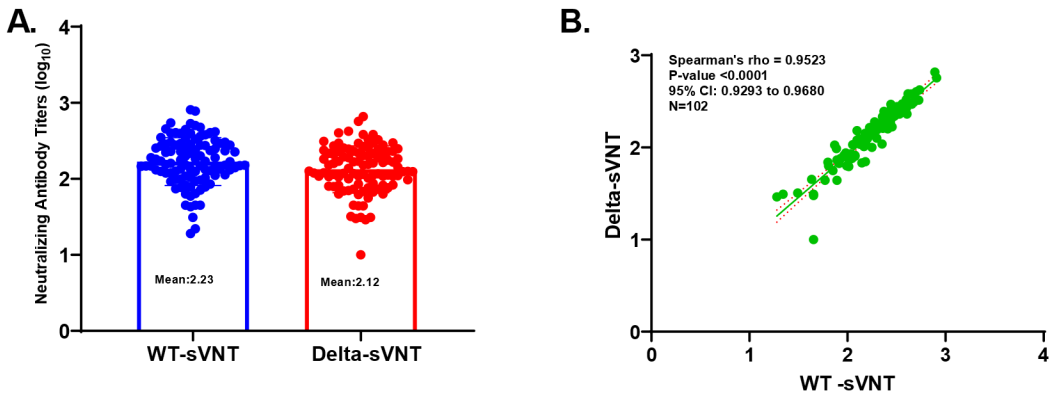

Figure 20. Correlation and simple linear regression analysis of WT-sVNT-EC_{50} and Delta-sVNT-EC_{50}. A.) Depiction of the log EC_{50} neutralizing antibody titers and means for WT-sVNT and Delta-sVNT. B.) Post-vaccination sample panel correlation between WT-sVNT (n=102) and Delta-sVNT (n=102). Spearman's rho, p-value, linear regression line (solid line), and 95% CI (dashed line).

The EC_{80} means for the 1- month post-vaccination samples of the WT-sVNT and Delta-sVNT are displayed in Figure 21A. The mean of the EC_{80} values for WT-sVNT (1.76) and the Delta-sVNT mean (1.65) were very similar. A correlation analysis was used to compare the EC_{80} neutralizing antibody titers determined by the WT-sVNT and Delta-sVNT. The Spearman's rho and simple linear regression analysis was performed for the WT-sVNT (n=102) vs the Delta-sVNT (n=102; Figure 21B). The EC_{80} neutralizing antibody titers determined by the WT-sVNT and Delta-sVNT showed a very strong positive correlation (Spearman's rho = 0.9535; p-value <0.0001 and 95% CI: 0.9310 to 0.9687). The positive correlation is just as strong between the WT-sVNT vs Delta-sVNT at the EC_{50} neutralizing antibody titer as the EC_{80} neutralizing antibody titer.

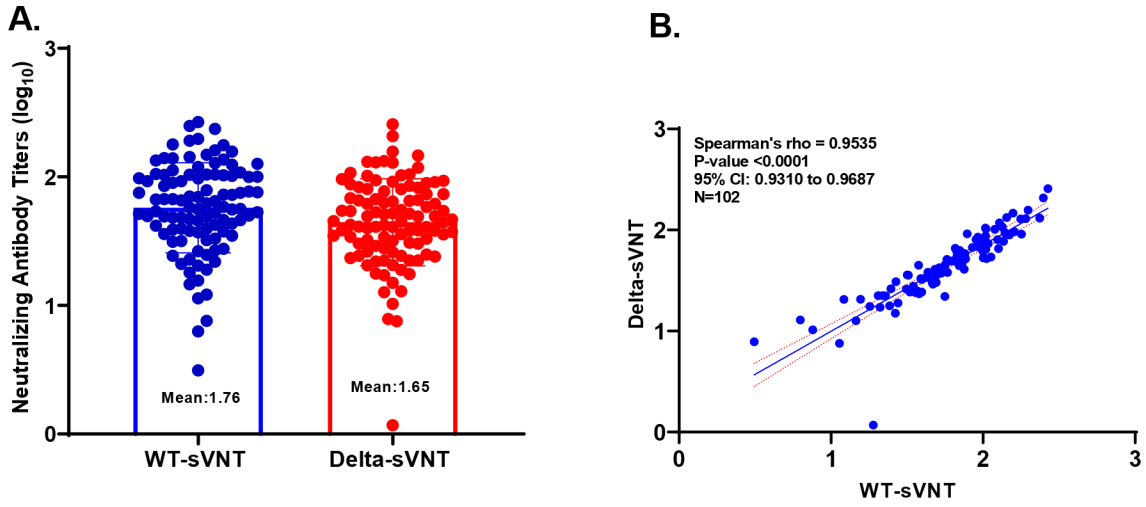

Figure 21. Correlation and simple linear regression analysis of WT-sVNT-EC$_{80}$ and Delta-sVNT-EC$_{80}$. A.) Depiction of the log EC$_{80}$ neutralizing antibody titers and means for WT-sVNT and Delta-sVNT. B.) Post-vaccination sample panel correlation between WT-sVNT (n=102) and Delta-sVNT (n=102). Spearman's rho, p-value, linear regression line (solid line), and 95% CI (dashed line).

The EC$_{50}$ neutralizing antibody titers for the Delta-sVNT was compared to the Delta-PNA results for the same cohort of 1-month post-vaccination samples (n=36; Figure 22A). The mean EC$_{50}$ neutralizing antibody titer for Delta-PNA is higher (2.47) than the titer for the Delta-sVNT (2.12). A correlation analysis was used to compare the EC$_{50}$ neutralizing antibody titers. The Spearman's rho and simple linear regression analysis was performed for both assays (Figure 22B). The EC$_{50}$ neutralizing antibody titers determined by Delta-sVNT and Delta-PNA showed a moderate positive correlation (Spearman's rho = 0.6306; p-value <0.0001 and 95% CI: 0.3724 to 0.7982).

Interestingly, the correlation is stronger between the WT-sVNT/PNA than the Delta-sVNT/PNA.

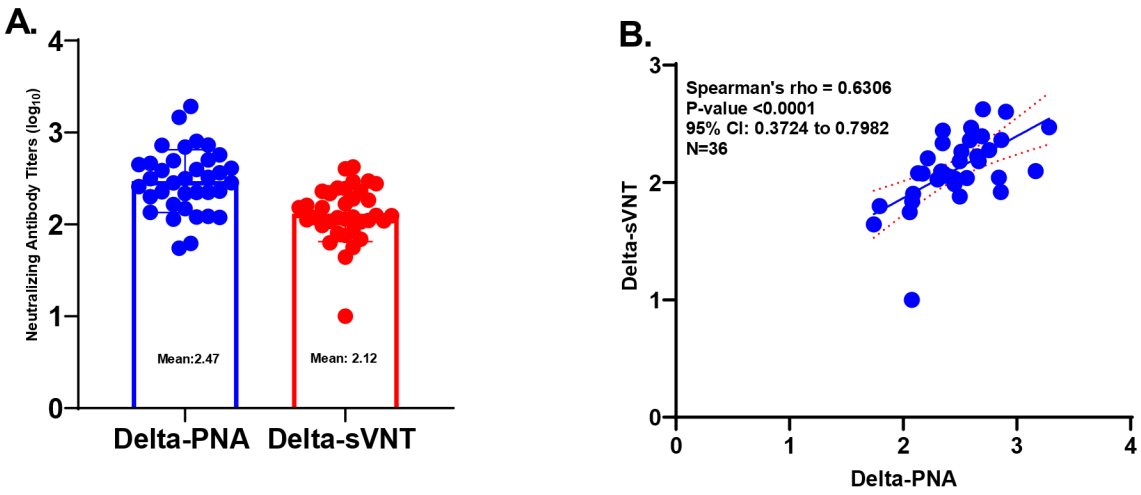

Figure 22. Correlation and simple linear regression analysis of Delta-sVNT and Delta-PNA. A.) Depiction of the log EC_{50} neutralizing antibody titers and means for Delta-PNA and Delta-sVNT. B.) Post-vaccination sample panel correlation between Delta-PNA (n=36) and Delta-sVNT (n=36). Spearman's rho, p-value, linear regression line (solid line), and 95% CI (dashed line).

An assay method comparison test was used to compare the EC_{50} neutralizing antibody titers determined by MN, PNA, and the sVNT. A Bland-Altman analysis was performed for all three assays using the same cohort of 1-month post-vaccination samples (n=36; Figure 23A-C). The WT-sVNT compared to the WT-MN had a close bias zero [bias = 0.07382; SD of bias = 0.2673 and 95% limit of agreement (LoA): -0.4501 to 0.5977; Figure 23]. The WT-sVNT compared to the WT-PNA had a bias further away from zero (bias = 0.5543; SD of bias=0.1703 and 95% LoA: 0.2206 to 0.8880). The WT-PNA compared to the WT-MN had the furthest bias from zero of all three comparisons (bias = 0.6281; SD of bias = 0.3069 and 95% LoA: 1.230 to 0.02664). Interestingly, the

WT-sVNT and the gold standard MN methods had the closest bias to zero, which indicates both methods are systemically producing the same results.

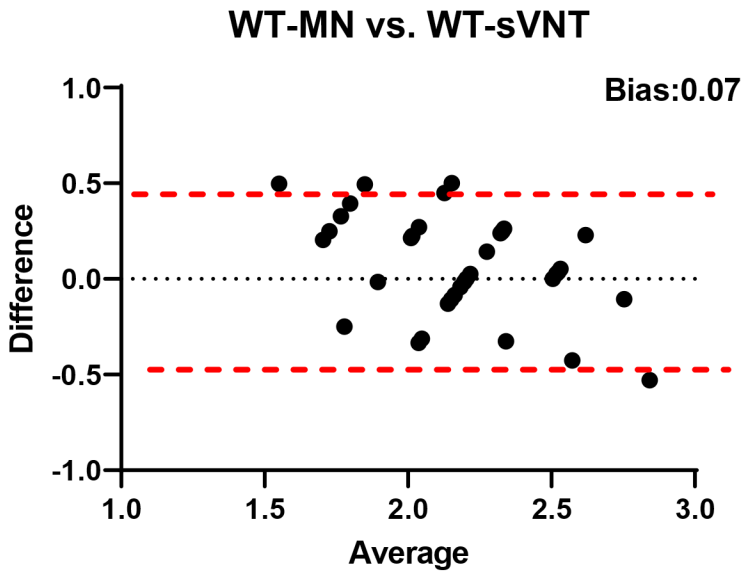

Figure 23. Bland-Atlman plot results of WT-sVNT, WT-MN and WT-PNA to compare assay methods. Plotted on the Y-axis is the difference and X-axis is the average of EC_{50} neutralizing antibodies against the SARS-CoV-2 WT S1-RBD. 95% LoA (dashed line) WT-MN (n=36), WT-PNA (n=36) and WT-sVNT (n=36).

DISCUSSION

Neutralizing antibody titers have been considered one of the measurable correlates of protection needed to determine the threshold of protective immunity against COVID-19. A reliable sVNT method using a rapid and automated platform to detect and quantify neutralizing antibody titers could serve as an indicator of protective immunity. Simple Plex™ immunoassays are automated, self-contained, and require minimal user involvement once a cartridge is loaded with reagents and samples. Additionally, the Simple Plex™ sVNT is easily modified to test sera for neutralizing antibody titers against emerging variants.

In this study, we proposed that running a sVNT on a rapid and automated Simple Plex™ immunoassay platform would render comparable neutralizing antibody titers to other neutralization assays. MNs, and similar tests like PRNTs, are considered gold standard neutralization assays because they utilize the WT live virus and are cell-based. However, a limitation for SARS-CoV-2 is these VNAs must be performed in a BSL-3 laboratory and they take multiple days to complete. PNAs can be run in a BSL-2 laboratory, but it still takes multiple days to generate results. The current sVNTs do not require cells, live or pseudo virus, can be performed in a BSL-2 lab, and can produce results in just hours. The Simple Plex™ sVNT provides the added advantage of a more rapid and automated assay compared to the current ELISA-based sVNT. We also wanted to determine the ability of the automated sVNT to detect neutralizing antibodies against multiple emerging SARS-CoV-2 variants. An advantage of our SARS-CoV-2 sVNT is the relative ease of switching S1-RBD capture antigens depending upon the variant of interest.

Here we developed and evaluated a sVNT performed on the Simple Plex™ rapid and automated immunoassay platform. The test achieves 100% sensitivity and 99-100% specificity and when compared to a gold standard MN cell-based assay, the sVNT shows a strong correlation and low bias in assay method comparison. Even though there were differences in the EC_{50} neutralizing antibody titers for some VNAs, all three assays had a good overall positive correlation. These results are similar to studies that evaluated commercially available sVNT [Tan et al. (2020) and Valcourt et al. (2021)] and supports our hypothesis that similar titers of neutralizing antibodies can be detected using the Simple Plex™ sVNT as compared to more traditional cell-based neutralization assays. The gold standard MN assay determined EC_{50} neutralizing antibody titers were not significantly different compared to the WT-sVNT and Delta-sVNT, which was further verified with correlation analysis and Bland-Altman bias agreement.

A current limitation in all sVNTs is that only neutralizing activity between the S1-RBD-hACE2 interaction can be detected. Not all neutralizing antibodies are RBD-binding antibodies and may have neutralizing activity to other epitopes on the SARS-CoV-2 virion that are not detected by the sVNT. While the sVNT cannot detect all neutralizing activity, the most dominant neutralizing antibody response involves the S1-RBD. The limitation of sVNT was highlighted by Hoffman et al. (2022) who determined that the commercial sVNT are suitable to detect neutralizing antibodies, but confirmatory testing by PRNT is still needed (Hofmann et al. 2022). While the sVNT may never be able to completely replace cell-based assays that use live virus, our results and others demonstrate the utility and comparability of the sVNT to gold standard assays.

In the current project, only one sample set was tested with known vaccination status of the patient samples. To further validate our results, more sample sets from different studies should be evaluated on the automated sVNT. A larger cohort of samples should also be used for additional head-to-head comparisons of the various VNAs. In the current study, only one sample set, one time point and one vaccine was analyzed, so comparing the automated and rapid sVNT to a MN and PNA with more sample sets, at different time points and multiple vaccines with samples of unknown vaccination status would need to be tested to ensure that the findings are reproducible. Additional studies should continue to evaluate the automated and rapid sVNTs ability to detect neutralizing activity against additional emerging variants such as the Omicron variant (B.1.1.529) and see if the MN and PNA render similar results to further demonstrate the robustness of the automated rapid SARS-CoV-2 sVNT.

In summary, this highly sensitive and specific sVNT shows strong correlation to gold standard VNAs and can be used in future studies for monitoring levels of neutralizing antibodies. Current commercially available sVNTs are rapid, but not automated, so the Simple Plex^{TM} sVNT developed here will be advantageous for increasing the ease and throughput for determining SARS-CoV-2 neutralizing antibody titers. This could lead to the possibility that in the future, clinics might be able to implement this assay for routine monitoring of SARS-CoV-2 neutralizing antibody titers to help inform the need for additional vaccination to protect the population from COVID-19.

SUPPLEMENTAL TABLES

S1. ROC analysis data for WT-sVNT

	Sensitivity%	95% CI	Sensitivity%	95% CI	Likelihood ratio
> 0.03000	100.0	96.40% to 100.0%	47.78	41.02% to 54.63%	1.915
> 0.1900	100.0	96.40% to 100.0%	48.28	41.50% to 55.12%	1.933
> 0.3450	100.0	96.40% to 100.0%	48.77	41.98% to 55.60%	1.952
> 0.4300	100.0	96.40% to 100.0%	49.26	42.46% to 56.09%	1.971
> 0.5238	100.0	96.40% to 100.0%	49.75	42.94% to 56.57%	1.990
> 0.5862	100.0	96.40% to 100.0%	50.25	43.43% to 57.06%	2.010
> 0.6225	100.0	96.40% to 100.0%	50.74	43.91% to 57.54%	2.030
> 0.6325	100.0	96.40% to 100.0%	51.23	44.40% to 58.02%	2.051
> 0.6530	100.0	96.40% to 100.0%	51.72	44.88% to 58.50%	2.071
> 0.7455	100.0	96.40% to 100.0%	52.22	45.37% to 58.98%	2.093
> 0.8650	100.0	96.40% to 100.0%	52.71	45.85% to 59.46%	2.115
> 0.9750	100.0	96.40% to 100.0%	53.20	46.34% to 59.94%	2.137
> 1.071	100.0	96.40% to 100.0%	53.69	46.83% to 60.42%	2.160
> 1.131	100.0	96.40% to 100.0%	54.19	47.32% to 60.90%	2.183
> 1.190	100.0	96.40% to 100.0%	54.68	47.81% to 61.38%	2.207
> 1.229	100.0	96.40% to 100.0%	55.17	48.30% to 61.85%	2.231
> 1.284	100.0	96.40% to 100.0%	55.67	48.79% to 62.33%	2.256
> 1.340	100.0	96.40% to 100.0%	56.16	49.28% to 62.81%	2.281
> 1.365	100.0	96.40% to 100.0%	56.65	49.77% to 63.28%	2.307
> 1.490	100.0	96.40% to 100.0%	57.14	50.26% to 63.76%	2.333
> 1.610	100.0	96.40% to 100.0%	57.64	50.76% to 64.23%	2.360
> 1.640	100.0	96.40% to 100.0%	58.13	51.25% to 64.70%	2.388
> 1.676	100.0	96.40% to 100.0%	58.62	51.75% to 65.17%	2.417
> 1.731	100.0	96.40% to 100.0%	59.11	52.24% to 65.65%	2.446
> 1.780	100.0	96.40% to 100.0%	59.61	52.74% to 66.12%	2.476
> 1.840	100.0	96.40% to 100.0%	60.10	53.23% to 66.59%	2.506
> 1.895	100.0	96.40% to 100.0%	60.59	53.73% to 67.06%	2.538
> 1.930	100.0	96.40% to 100.0%	61.08	54.23% to 67.53%	2.570
> 2.085	100.0	96.40% to 100.0%	61.58	54.73% to 67.99%	2.603
> 2.270	100.0	96.40% to 100.0%	62.07	55.23% to 68.46%	2.636
> 2.455	100.0	96.40% to 100.0%	62.56	55.73% to 68.93%	2.671
> 2.610	100.0	96.40% to 100.0%	63.05	56.23% to 69.39%	2.707
> 2.650	100.0	96.40% to 100.0%	63.55	56.73% to 69.86%	2.743
> 2.680	100.0	96.40% to 100.0%	64.04	57.23% to 70.32%	2.781
> 2.850	100.0	96.40% to 100.0%	64.53	57.74% to 70.79%	2.819
> 3.010	100.0	96.40% to 100.0%	65.02	58.24% to 71.25%	2.859
> 3.055	100.0	96.40% to 100.0%	65.52	58.75% to 71.71%	2.900
> 3.155	100.0	96.40% to 100.0%	66.01	59.25% to 72.17%	2.942
> 3.306	100.0	96.40% to 100.0%	66.50	59.76% to 72.64%	2.985
> 3.401	100.0	96.40% to 100.0%	67.00	60.26% to 73.10%	3.030
> 3.640	100.0	96.40% to 100.0%	67.49	60.77% to 73.55%	3.076
> 3.875	100.0	96.40% to 100.0%	67.98	61.28% to 74.01%	3.123
> 3.927	100.0	96.40% to 100.0%	68.47	61.79% to 74.47%	3.172
> 4.024	100.0	96.40% to 100.0%	68.97	62.30% to 74.93%	3.222
> 4.187	100.0	96.40% to 100.0%	69.46	62.81% to 75.38%	3.274

> 4.444	100.0	96.40% to 100.0%	69.95	63.32% to 75.84%	3.328
> 4.673	100.0	96.40% to 100.0%	70.44	63.83% to 76.29%	3.383
> 4.999	100.0	96.40% to 100.0%	70.94	64.35% to 76.75%	3.441
> 5.248	100.0	96.40% to 100.0%	71.43	64.86% to 77.20%	3.500
> 5.289	100.0	96.40% to 100.0%	71.92	65.38% to 77.65%	3.561
> 5.336	100.0	96.40% to 100.0%	72.41	65.89% to 78.10%	3.625
> 5.400	100.0	96.40% to 100.0%	72.91	66.41% to 78.55%	3.691
> 5.480	100.0	96.40% to 100.0%	73.40	66.93% to 79.00%	3.759
> 5.525	100.0	96.40% to 100.0%	73.89	67.45% to 79.45%	3.830
> 5.560	100.0	96.40% to 100.0%	74.38	67.97% to 79.90%	3.904
> 5.705	100.0	96.40% to 100.0%	74.88	68.49% to 80.34%	3.980
> 5.910	100.0	96.40% to 100.0%	75.37	69.01% to 80.79%	4.060
> 6.015	100.0	96.40% to 100.0%	75.86	69.53% to 81.23%	4.143
> 6.125	100.0	96.40% to 100.0%	76.35	70.05% to 81.68%	4.229
> 6.215	100.0	96.40% to 100.0%	76.85	70.58% to 82.12%	4.319
> 6.230	100.0	96.40% to 100.0%	77.34	71.10% to 82.56%	4.413
> 6.254	100.0	96.40% to 100.0%	77.83	71.63% to 83.00%	4.511
> 6.298	100.0	96.40% to 100.0%	78.33	72.16% to 83.44%	4.614
> 6.458	100.0	96.40% to 100.0%	78.82	72.69% to 83.88%	4.721
> 6.624	100.0	96.40% to 100.0%	79.31	73.22% to 84.31%	4.833
> 6.735	100.0	96.40% to 100.0%	79.80	73.75% to 84.75%	4.951
> 6.890	100.0	96.40% to 100.0%	80.30	74.28% to 85.18%	5.075
> 6.991	100.0	96.40% to 100.0%	80.79	74.82% to 85.62%	5.205
> 7.056	100.0	96.40% to 100.0%	81.28	75.35% to 86.05%	5.342
> 7.130	100.0	96.40% to 100.0%	81.77	75.89% to 86.48%	5.486
> 7.343	100.0	96.40% to 100.0%	82.27	76.43% to 86.91%	5.639
> 7.578	100.0	96.40% to 100.0%	82.76	76.97% to 87.33%	5.800
> 7.700	100.0	96.40% to 100.0%	83.25	77.51% to 87.76%	5.971
> 7.794	100.0	96.40% to 100.0%	83.74	78.05% to 88.18%	6.152
> 7.829	100.0	96.40% to 100.0%	84.24	78.59% to 88.61%	6.344
> 7.845	100.0	96.40% to 100.0%	84.73	79.14% to 89.03%	6.548
> 7.970	100.0	96.40% to 100.0%	85.22	79.69% to 89.45%	6.767
> 8.311	100.0	96.40% to 100.0%	85.71	80.24% to 89.87%	7.000
> 8.811	100.0	96.40% to 100.0%	86.21	80.79% to 90.28%	7.250
> 9.305	100.0	96.40% to 100.0%	86.70	81.34% to 90.70%	7.519
> 9.560	100.0	96.40% to 100.0%	87.19	81.90% to 91.11%	7.808
> 9.655	100.0	96.40% to 100.0%	87.68	82.45% to 91.52%	8.120
> 9.746	100.0	96.40% to 100.0%	88.18	83.01% to 91.93%	8.458
> 9.821	100.0	96.40% to 100.0%	88.67	83.57% to 92.33%	8.826
> 9.920	100.0	96.40% to 100.0%	89.16	84.14% to 92.73%	9.227
> 10.00	100.0	96.40% to 100.0%	89.66	84.70% to 93.13%	9.667
> 10.06	100.0	96.40% to 100.0%	90.15	85.27% to 93.53%	10.15
> 10.17	100.0	96.40% to 100.0%	90.64	85.85% to 93.93%	10.68
> 10.27	100.0	96.40% to 100.0%	91.13	86.42% to 94.32%	11.28
> 10.62	100.0	96.40% to 100.0%	91.63	87.00% to 94.71%	11.94
> 11.18	100.0	96.40% to 100.0%	92.12	87.58% to 95.09%	12.69
> 11.56	100.0	96.40% to 100.0%	92.61	88.17% to 95.47%	13.53
> 11.93	100.0	96.40% to 100.0%	93.10	88.76% to 95.85%	14.50
> 12.26	100.0	96.40% to 100.0%	93.60	89.35% to 96.22%	15.62

> 12.37	100.0	96.40% to 100.0%	94.09	89.95% to 96.59%	16.92
> 12.39	100.0	96.40% to 100.0%	94.58	90.56% to 96.95%	18.45
> 12.50	100.0	96.40% to 100.0%	95.07	91.17% to 97.30%	20.30
> 12.92	100.0	96.40% to 100.0%	95.57	91.79% to 97.65%	22.56
> 14.14	100.0	96.40% to 100.0%	96.06	92.42% to 97.99%	25.38
> 15.79	100.0	96.40% to 100.0%	96.55	93.05% to 98.32%	29.00
> 17.79	100.0	96.40% to 100.0%	97.04	93.70% to 98.64%	33.83
> 19.96	100.0	96.40% to 100.0%	97.54	94.36% to 98.94%	40.60
> 21.56	100.0	96.40% to 100.0%	98.03	95.04% to 99.23%	50.75
> 22.81	100.0	96.40% to 100.0%	98.52	95.75% to 99.60%	67.67
> 24.30	100.0	96.40% to 100.0%	99.01	96.48% to 99.82%	101.5
> 25.47	100.0	96.40% to 100.0%	99.51	97.26% to 99.97%	203.0
> 53.76	100.0	96.40% to 100.0%	100.0	98.14% to 100.0%	
> 84.35	99.03	94.70% to 99.95%	100.0	98.14% to 100.0%	
> 87.18	98.06	93.19% to 99.65%	100.0	98.14% to 100.0%	
> 87.74	97.09	91.78% to 99.21%	100.0	98.14% to 100.0%	
> 89.29	96.12	90.44% to 98.48%	100.0	98.14% to 100.0%	
> 90.70	95.15	89.14% to 97.91%	100.0	98.14% to 100.0%	
> 90.99	94.17	87.87% to 97.30%	100.0	98.14% to 100.0%	
> 91.81	93.20	86.63% to 96.67%	100.0	98.14% to 100.0%	
> 93.03	92.23	85.42% to 96.01%	100.0	98.14% to 100.0%	
> 93.84	91.26	84.22% to 95.33%	100.0	98.14% to 100.0%	
> 94.13	90.29	83.04% to 94.64%	100.0	98.14% to 100.0%	
> 94.52	89.32	81.88% to 93.93%	100.0	98.14% to 100.0%	
> 94.91	88.35	80.73% to 93.21%	100.0	98.14% to 100.0%	
> 95.29	87.38	79.60% to 92.47%	100.0	98.14% to 100.0%	
> 95.72	86.41	78.47% to 91.73%	100.0	98.14% to 100.0%	
> 95.78	84.47	76.25% to 90.21%	100.0	98.14% to 100.0%	
> 95.86	83.50	75.15% to 89.43%	100.0	98.14% to 100.0%	
> 95.95	82.52	74.06% to 88.65%	100.0	98.14% to 100.0%	
> 96.03	81.55	72.98% to 87.86%	100.0	98.14% to 100.0%	
> 96.15	80.58	71.90% to 87.06%	100.0	98.14% to 100.0%	
> 96.21	79.61	70.83% to 86.26%	100.0	98.14% to 100.0%	
> 96.43	78.64	69.77% to 85.45%	100.0	98.14% to 100.0%	
> 96.71	77.67	68.72% to 84.63%	100.0	98.14% to 100.0%	
> 96.80	76.70	67.67% to 83.81%	100.0	98.14% to 100.0%	
> 96.84	75.73	66.62% to 82.98%	100.0	98.14% to 100.0%	
> 96.85	74.76	65.58% to 82.15%	100.0	98.14% to 100.0%	
> 97.00	73.79	64.55% to 81.31%	100.0	98.14% to 100.0%	
> 97.14	72.82	63.52% to 80.47%	100.0	98.14% to 100.0%	
> 97.16	71.84	62.49% to 79.62%	100.0	98.14% to 100.0%	
> 97.23	70.87	61.48% to 78.77%	100.0	98.14% to 100.0%	
> 97.37	69.90	60.46% to 77.91%	100.0	98.14% to 100.0%	
> 97.49	68.93	59.45% to 77.05%	100.0	98.14% to 100.0%	
> 97.56	67.96	58.44% to 76.19%	100.0	98.14% to 100.0%	
> 97.61	66.99	57.44% to 75.32%	100.0	98.14% to 100.0%	
> 97.67	66.02	56.44% to 74.44%	100.0	98.14% to 100.0%	
> 97.73	65.05	55.45% to 73.56%	100.0	98.14% to 100.0%	
> 97.77	64.08	54.46% to 72.68%	100.0	98.14% to 100.0%	

> 97.79	63.11	53.47% to 71.80%	100.0	98.14% to 100.0%	
> 97.81	61.17	51.51% to 70.01%	100.0	98.14% to 100.0%	
> 97.84	60.19	50.54% to 69.12%	100.0	98.14% to 100.0%	
> 97.88	59.22	49.57% to 68.22%	100.0	98.14% to 100.0%	
> 97.90	58.25	48.60% to 67.31%	100.0	98.14% to 100.0%	
> 97.96	57.28	47.64% to 66.40%	100.0	98.14% to 100.0%	
> 98.02	56.31	46.68% to 65.49%	100.0	98.14% to 100.0%	
> 98.07	54.37	44.77% to 63.66%	100.0	98.14% to 100.0%	
> 98.13	53.40	43.82% to 62.74%	100.0	98.14% to 100.0%	
> 98.18	52.43	42.87% to 61.81%	100.0	98.14% to 100.0%	
> 98.25	51.46	41.93% to 60.88%	100.0	98.14% to 100.0%	
> 98.33	49.51	40.05% to 59.01%	100.0	98.14% to 100.0%	
> 98.37	48.54	39.12% to 58.07%	100.0	98.14% to 100.0%	
> 98.39	47.57	38.19% to 57.13%	100.0	98.14% to 100.0%	
> 98.40	46.60	37.26% to 56.18%	100.0	98.14% to 100.0%	
> 98.41	45.63	36.34% to 55.23%	100.0	98.14% to 100.0%	
> 98.45	44.66	35.42% to 54.28%	100.0	98.14% to 100.0%	
> 98.49	43.69	34.51% to 53.32%	100.0	98.14% to 100.0%	
> 98.53	42.72	33.60% to 52.36%	100.0	98.14% to 100.0%	
> 98.57	41.75	32.69% to 51.40%	100.0	98.14% to 100.0%	
> 98.59	40.78	31.78% to 50.43%	100.0	98.14% to 100.0%	
> 98.61	39.81	30.88% to 49.46%	100.0	98.14% to 100.0%	
> 98.65	38.83	29.99% to 48.49%	100.0	98.14% to 100.0%	
> 98.68	37.86	29.09% to 47.51%	100.0	98.14% to 100.0%	
> 98.71	36.89	28.20% to 46.53%	100.0	98.14% to 100.0%	
> 98.77	35.92	27.32% to 45.54%	100.0	98.14% to 100.0%	
> 98.85	34.95	26.44% to 44.55%	100.0	98.14% to 100.0%	
> 98.89	33.98	25.56% to 43.56%	100.0	98.14% to 100.0%	
> 98.93	32.04	23.81% to 41.56%	100.0	98.14% to 100.0%	
> 98.98	30.10	22.09% to 39.54%	100.0	98.14% to 100.0%	
> 98.99	28.16	20.38% to 37.51%	100.0	98.14% to 100.0%	
> 99.03	27.18	19.53% to 36.48%	100.0	98.14% to 100.0%	
> 99.08	25.24	17.85% to 34.42%	100.0	98.14% to 100.0%	
> 99.10	24.27	17.02% to 33.38%	100.0	98.14% to 100.0%	
> 99.11	23.30	16.19% to 32.33%	100.0	98.14% to 100.0%	
> 99.14	22.33	15.37% to 31.28%	100.0	98.14% to 100.0%	
> 99.16	21.36	14.55% to 30.23%	100.0	98.14% to 100.0%	
> 99.18	20.39	13.74% to 29.17%	100.0	98.14% to 100.0%	
> 99.22	18.45	12.14% to 27.02%	100.0	98.14% to 100.0%	
> 99.27	17.48	11.35% to 25.94%	100.0	98.14% to 100.0%	
> 99.29	16.50	10.57% to 24.85%	100.0	98.14% to 100.0%	
> 99.32	15.53	9.794% to 23.75%	100.0	98.14% to 100.0%	
> 99.35	14.56	9.028% to 22.65%	100.0	98.14% to 100.0%	
> 99.37	13.59	8.272% to 21.53%	100.0	98.14% to 100.0%	
> 99.38	12.62	7.526% to 20.40%	100.0	98.14% to 100.0%	
> 99.40	11.65	6.792% to 19.27%	100.0	98.14% to 100.0%	
> 99.43	10.68	6.069% to 18.12%	100.0	98.14% to 100.0%	
> 99.47	9.709	5.359% to 16.96%	100.0	98.14% to 100.0%	
> 99.49	8.738	4.665% to 15.78%	100.0	98.14% to 100.0%	

> 99.53	6.796	3.331% to 13.37%	100.0	98.14% to 100.0%	
> 99.57	5.825	2.697% to 12.13%	100.0	98.14% to 100.0%	
> 99.58	4.854	2.091% to 10.86%	100.0	98.14% to 100.0%	
> 99.59	3.883	1.520% to 9.563%	100.0	98.14% to 100.0%	
> 99.60	2.913	0.7939% to 8.216%	100.0	98.14% to 100.0%	
> 99.61	1.942	0.3450% to 6.805%	100.0	98.14% to 100.0%	
> 99.68	0.9709	0.04980% to 5.296%	100.0	98.14% to 100.0%	

Abbreviations: CI: Confidence Interval.

S2. ROC analysis data for Delta-sVNT

	Sensitivity%	95% CI	Specificity%	95% CI	Likelihood ratio
> 0.09500	100.0	96.40% to 100.0%	29.06	23.25% to 35.65%	1.410
> 0.2250	100.0	96.40% to 100.0%	29.56	23.71% to 36.17%	1.420
> 0.3400	100.0	96.40% to 100.0%	30.05	24.16% to 36.68%	1.430
> 0.5150	100.0	96.40% to 100.0%	30.54	24.62% to 37.19%	1.440
> 0.6911	100.0	96.40% to 100.0%	31.03	25.07% to 37.70%	1.450
> 0.8111	100.0	96.40% to 100.0%	31.53	25.53% to 38.21%	1.460
> 0.8650	100.0	96.40% to 100.0%	32.02	25.99% to 38.72%	1.471
> 0.8850	100.0	96.40% to 100.0%	32.51	26.45% to 39.23%	1.482
> 0.9600	100.0	96.40% to 100.0%	33.00	26.90% to 39.74%	1.493
> 1.155	100.0	96.40% to 100.0%	33.50	27.36% to 40.24%	1.504
> 1.302	100.0	96.40% to 100.0%	33.99	27.83% to 40.75%	1.515
> 1.367	100.0	96.40% to 100.0%	34.48	28.29% to 41.25%	1.526
> 1.430	100.0	96.40% to 100.0%	34.98	28.75% to 41.76%	1.538
> 1.480	100.0	96.40% to 100.0%	35.47	29.21% to 42.26%	1.550
> 1.565	100.0	96.40% to 100.0%	35.96	29.68% to 42.77%	1.562
> 1.625	100.0	96.40% to 100.0%	36.45	30.14% to 43.27%	1.574
> 1.645	100.0	96.40% to 100.0%	36.95	30.61% to 43.77%	1.586
> 1.665	100.0	96.40% to 100.0%	37.44	31.07% to 44.27%	1.598
> 1.684	100.0	96.40% to 100.0%	37.93	31.54% to 44.77%	1.611
> 1.719	100.0	96.40% to 100.0%	38.42	32.01% to 45.27%	1.624
> 1.750	100.0	96.40% to 100.0%	38.92	32.47% to 45.77%	1.637
> 1.828	100.0	96.40% to 100.0%	39.41	32.94% to 46.27%	1.650
> 1.928	100.0	96.40% to 100.0%	39.90	33.41% to 46.77%	1.664
> 2.006	100.0	96.40% to 100.0%	40.39	33.88% to 47.26%	1.678
> 2.151	100.0	96.40% to 100.0%	40.89	34.35% to 47.76%	1.692
> 2.255	100.0	96.40% to 100.0%	41.38	34.83% to 48.25%	1.706
> 2.265	100.0	96.40% to 100.0%	41.87	35.30% to 48.75%	1.720
> 2.305	100.0	96.40% to 100.0%	42.36	35.77% to 49.24%	1.735
> 2.365	100.0	96.40% to 100.0%	42.86	36.24% to 49.74%	1.750
> 2.398	100.0	96.40% to 100.0%	43.35	36.72% to 50.23%	1.765
> 2.418	100.0	96.40% to 100.0%	43.84	37.19% to 50.72%	1.781
> 2.550	100.0	96.40% to 100.0%	44.33	37.67% to 51.21%	1.796
> 2.705	100.0	96.40% to 100.0%	44.83	38.15% to 51.70%	1.813
> 2.785	100.0	96.40% to 100.0%	45.32	38.62% to 52.19%	1.829
> 2.850	100.0	96.40% to 100.0%	45.81	39.10% to 52.68%	1.845
> 2.940	100.0	96.40% to 100.0%	46.31	39.58% to 53.17%	1.862

> 3.063	100.0	96.40% to 100.0%	46.80	40.06% to 53.66%	1.880
> 3.218	100.0	96.40% to 100.0%	47.29	40.54% to 54.15%	1.897
> 3.520	100.0	96.40% to 100.0%	47.78	41.02% to 54.63%	1.915
> 3.760	100.0	96.40% to 100.0%	48.28	41.50% to 55.12%	1.933
> 3.805	100.0	96.40% to 100.0%	48.77	41.98% to 55.60%	1.952
> 3.845	100.0	96.40% to 100.0%	49.26	42.46% to 56.09%	1.971
> 3.895	100.0	96.40% to 100.0%	49.75	42.94% to 56.57%	1.990
> 3.940	100.0	96.40% to 100.0%	50.25	43.43% to 57.06%	2.010
> 4.080	100.0	96.40% to 100.0%	50.74	43.91% to 57.54%	2.030
> 4.266	100.0	96.40% to 100.0%	51.23	44.40% to 58.02%	2.051
> 4.466	100.0	96.40% to 100.0%	51.72	44.88% to 58.50%	2.071
> 4.620	100.0	96.40% to 100.0%	52.22	45.37% to 58.98%	2.093
> 4.670	100.0	96.40% to 100.0%	52.71	45.85% to 59.46%	2.115
> 4.695	100.0	96.40% to 100.0%	53.20	46.34% to 59.94%	2.137
> 4.705	100.0	96.40% to 100.0%	53.69	46.83% to 60.42%	2.160
> 4.744	100.0	96.40% to 100.0%	54.19	47.32% to 60.90%	2.183
> 4.779	100.0	96.40% to 100.0%	54.68	47.81% to 61.38%	2.207
> 4.795	100.0	96.40% to 100.0%	55.17	48.30% to 61.85%	2.231
> 4.820	100.0	96.40% to 100.0%	56.16	49.28% to 62.81%	2.281
> 4.835	100.0	96.40% to 100.0%	56.65	49.77% to 63.28%	2.307
> 4.855	100.0	96.40% to 100.0%	57.14	50.26% to 63.76%	2.333
> 4.905	100.0	96.40% to 100.0%	57.64	50.76% to 64.23%	2.360
> 4.998	100.0	96.40% to 100.0%	58.13	51.25% to 64.70%	2.388
> 5.092	100.0	96.40% to 100.0%	58.62	51.75% to 65.17%	2.417
> 5.214	100.0	96.40% to 100.0%	59.11	52.24% to 65.65%	2.446
> 5.320	100.0	96.40% to 100.0%	59.61	52.74% to 66.12%	2.476
> 5.375	100.0	96.40% to 100.0%	60.10	53.23% to 66.59%	2.506
> 5.420	100.0	96.40% to 100.0%	60.59	53.73% to 67.06%	2.538
> 5.475	100.0	96.40% to 100.0%	61.08	54.23% to 67.53%	2.570
> 5.535	100.0	96.40% to 100.0%	61.58	54.73% to 67.99%	2.603
> 5.675	100.0	96.40% to 100.0%	62.56	55.73% to 68.93%	2.671
> 5.845	100.0	96.40% to 100.0%	63.05	56.23% to 69.39%	2.707
> 5.925	100.0	96.40% to 100.0%	63.55	56.73% to 69.86%	2.743
> 6.060	100.0	96.40% to 100.0%	64.04	57.23% to 70.32%	2.781
> 6.180	100.0	96.40% to 100.0%	64.53	57.74% to 70.79%	2.819
> 6.248	100.0	96.40% to 100.0%	65.02	58.24% to 71.25%	2.859
> 6.353	100.0	96.40% to 100.0%	65.52	58.75% to 71.71%	2.900
> 6.435	100.0	96.40% to 100.0%	66.01	59.25% to 72.17%	2.942
> 6.560	100.0	96.40% to 100.0%	66.50	59.76% to 72.64%	2.985
> 6.680	100.0	96.40% to 100.0%	67.00	60.26% to 73.10%	3.030
> 6.736	100.0	96.40% to 100.0%	67.49	60.77% to 73.55%	3.076
> 6.791	100.0	96.40% to 100.0%	67.98	61.28% to 74.01%	3.123
> 6.865	100.0	96.40% to 100.0%	68.47	61.79% to 74.47%	3.172
> 6.964	100.0	96.40% to 100.0%	68.97	62.30% to 74.93%	3.222
> 7.124	100.0	96.40% to 100.0%	69.46	62.81% to 75.38%	3.274
> 7.275	100.0	96.40% to 100.0%	69.95	63.32% to 75.84%	3.328
> 7.320	100.0	96.40% to 100.0%	70.44	63.83% to 76.29%	3.383
> 7.465	100.0	96.40% to 100.0%	70.94	64.35% to 76.75%	3.441
> 7.770	100.0	96.40% to 100.0%	71.43	64.86% to 77.20%	3.500

> 7.971	100.0	96.40% to 100.0%	71.92	65.38% to 77.65%	3.561
> 8.068	100.0	96.40% to 100.0%	72.41	65.89% to 78.10%	3.625
> 8.193	100.0	96.40% to 100.0%	72.91	66.41% to 78.55%	3.691
> 8.280	100.0	96.40% to 100.0%	73.40	66.93% to 79.00%	3.759
> 8.335	100.0	96.40% to 100.0%	73.89	67.45% to 79.45%	3.830
> 8.495	100.0	96.40% to 100.0%	74.38	67.97% to 79.90%	3.904
> 8.655	100.0	96.40% to 100.0%	74.88	68.49% to 80.34%	3.980
> 8.760	100.0	96.40% to 100.0%	75.37	69.01% to 80.79%	4.060
> 8.965	100.0	96.40% to 100.0%	75.86	69.53% to 81.23%	4.143
> 9.225	100.0	96.40% to 100.0%	76.35	70.05% to 81.68%	4.229
> 9.410	100.0	96.40% to 100.0%	76.85	70.58% to 82.12%	4.319
> 9.490	100.0	96.40% to 100.0%	77.34	71.10% to 82.56%	4.413
> 9.560	100.0	96.40% to 100.0%	77.83	71.63% to 83.00%	4.511
> 9.605	100.0	96.40% to 100.0%	78.33	72.16% to 83.44%	4.614
> 9.686	100.0	96.40% to 100.0%	78.82	72.69% to 83.88%	4.721
> 9.789	100.0	96.40% to 100.0%	79.31	73.22% to 84.31%	4.833
> 9.828	100.0	96.40% to 100.0%	79.80	73.75% to 84.75%	4.951
> 9.883	100.0	96.40% to 100.0%	80.30	74.28% to 85.18%	5.075
> 9.948	100.0	96.40% to 100.0%	80.79	74.82% to 85.62%	5.205
> 9.990	100.0	96.40% to 100.0%	81.28	75.35% to 86.05%	5.342
> 10.02	100.0	96.40% to 100.0%	81.77	75.89% to 86.48%	5.486
> 10.14	100.0	96.40% to 100.0%	82.27	76.43% to 86.91%	5.639
> 10.36	100.0	96.40% to 100.0%	82.76	76.97% to 87.33%	5.800
> 10.49	100.0	96.40% to 100.0%	83.74	78.05% to 88.18%	6.152
> 10.68	100.0	96.40% to 100.0%	84.24	78.59% to 88.61%	6.344
> 10.89	100.0	96.40% to 100.0%	84.73	79.14% to 89.03%	6.548
> 11.12	100.0	96.40% to 100.0%	85.22	79.69% to 89.45%	6.767
> 11.33	100.0	96.40% to 100.0%	85.71	80.24% to 89.87%	7.000
> 11.40	100.0	96.40% to 100.0%	86.21	80.79% to 90.28%	7.250
> 11.46	100.0	96.40% to 100.0%	86.70	81.34% to 90.70%	7.519
> 11.57	100.0	96.40% to 100.0%	87.19	81.90% to 91.11%	7.808
> 12.06	100.0	96.40% to 100.0%	87.68	82.45% to 91.52%	8.120
> 13.03	100.0	96.40% to 100.0%	88.18	83.01% to 91.93%	8.458
> 13.76	100.0	96.40% to 100.0%	88.67	83.57% to 92.33%	8.826
> 14.12	100.0	96.40% to 100.0%	89.16	84.14% to 92.73%	9.227
> 14.55	100.0	96.40% to 100.0%	89.66	84.70% to 93.13%	9.667
> 15.07	100.0	96.40% to 100.0%	90.15	85.27% to 93.53%	10.15
> 15.43	100.0	96.40% to 100.0%	90.64	85.85% to 93.93%	10.68
> 15.74	100.0	96.40% to 100.0%	91.13	86.42% to 94.32%	11.28
> 16.35	100.0	96.40% to 100.0%	91.63	87.00% to 94.71%	11.94
> 16.82	100.0	96.40% to 100.0%	92.12	87.58% to 95.09%	12.69
> 17.09	100.0	96.40% to 100.0%	92.61	88.17% to 95.47%	13.53
> 17.28	100.0	96.40% to 100.0%	93.10	88.76% to 95.85%	14.50
> 17.33	100.0	96.40% to 100.0%	93.60	89.35% to 96.22%	15.62
> 17.44	100.0	96.40% to 100.0%	94.09	89.95% to 96.59%	16.92
> 18.04	100.0	96.40% to 100.0%	94.58	90.56% to 96.95%	18.45
> 18.66	100.0	96.40% to 100.0%	95.07	91.17% to 97.30%	20.30
> 19.10	100.0	96.40% to 100.0%	95.57	91.79% to 97.65%	22.56
> 20.26	100.0	96.40% to 100.0%	96.06	92.42% to 97.99%	25.38

> 21.99	100.0	96.40% to 100.0%	96.55	93.05% to 98.32%	29.00
> 24.75	100.0	96.40% to 100.0%	97.04	93.70% to 98.64%	33.83
> 26.74	100.0	96.40% to 100.0%	97.54	94.36% to 98.94%	40.60
> 27.28	100.0	96.40% to 100.0%	98.03	95.04% to 99.23%	50.75
> 29.22	100.0	96.40% to 100.0%	98.52	95.75% to 99.60%	67.67
> 34.18	100.0	96.40% to 100.0%	99.01	96.48% to 99.82%	101.5
> 39.32	100.0	96.40% to 100.0%	99.51	97.26% to 99.97%	203.0
> 60.36	100.0	96.40% to 100.0%	100.0	98.14% to 100.0%	
> 81.23	99.03	94.70% to 99.95%	100.0	98.14% to 100.0%	
> 84.09	98.06	93.19% to 99.65%	100.0	98.14% to 100.0%	
> 85.67	97.09	91.78% to 99.21%	100.0	98.14% to 100.0%	
> 86.57	96.12	90.44% to 98.48%	100.0	98.14% to 100.0%	
> 88.29	95.15	89.14% to 97.91%	100.0	98.14% to 100.0%	
> 89.42	94.17	87.87% to 97.30%	100.0	98.14% to 100.0%	
> 90.71	93.20	86.63% to 96.67%	100.0	98.14% to 100.0%	
> 92.12	92.23	85.42% to 96.01%	100.0	98.14% to 100.0%	
> 92.89	91.26	84.22% to 95.33%	100.0	98.14% to 100.0%	
> 93.84	90.29	83.04% to 94.64%	100.0	98.14% to 100.0%	
> 94.19	89.32	81.88% to 93.93%	100.0	98.14% to 100.0%	
> 94.38	88.35	80.73% to 93.21%	100.0	98.14% to 100.0%	
> 94.63	87.38	79.60% to 92.47%	100.0	98.14% to 100.0%	
> 94.75	86.41	78.47% to 91.73%	100.0	98.14% to 100.0%	
> 94.90	85.44	77.35% to 90.97%	100.0	98.14% to 100.0%	
> 95.08	84.47	76.25% to 90.21%	100.0	98.14% to 100.0%	
> 95.40	82.52	74.06% to 88.65%	100.0	98.14% to 100.0%	
> 95.66	81.55	72.98% to 87.86%	100.0	98.14% to 100.0%	
> 95.73	80.58	71.90% to 87.06%	100.0	98.14% to 100.0%	
> 95.85	79.61	70.83% to 86.26%	100.0	98.14% to 100.0%	
> 95.92	78.64	69.77% to 85.45%	100.0	98.14% to 100.0%	
> 95.93	77.67	68.72% to 84.63%	100.0	98.14% to 100.0%	
> 96.04	76.70	67.67% to 83.81%	100.0	98.14% to 100.0%	
> 96.19	75.73	66.62% to 82.98%	100.0	98.14% to 100.0%	
> 96.24	74.76	65.58% to 82.15%	100.0	98.14% to 100.0%	
> 96.31	73.79	64.55% to 81.31%	100.0	98.14% to 100.0%	
> 96.41	72.82	63.52% to 80.47%	100.0	98.14% to 100.0%	
> 96.50	71.84	62.49% to 79.62%	100.0	98.14% to 100.0%	
> 96.55	70.87	61.48% to 78.77%	100.0	98.14% to 100.0%	
> 96.56	69.90	60.46% to 77.91%	100.0	98.14% to 100.0%	
> 96.59	68.93	59.45% to 77.05%	100.0	98.14% to 100.0%	
> 96.67	67.96	58.44% to 76.19%	100.0	98.14% to 100.0%	
> 96.80	66.99	57.44% to 75.32%	100.0	98.14% to 100.0%	
> 96.89	66.02	56.44% to 74.44%	100.0	98.14% to 100.0%	
> 97.08	65.05	55.45% to 73.56%	100.0	98.14% to 100.0%	
> 97.30	64.08	54.46% to 72.68%	100.0	98.14% to 100.0%	
> 97.40	63.11	53.47% to 71.80%	100.0	98.14% to 100.0%	
> 97.46	62.14	52.49% to 70.91%	100.0	98.14% to 100.0%	
> 97.47	61.17	51.51% to 70.01%	100.0	98.14% to 100.0%	
> 97.48	60.19	50.54% to 69.12%	100.0	98.14% to 100.0%	
> 97.49	58.25	48.60% to 67.31%	100.0	98.14% to 100.0%	

> 97.53	57.28	47.64% to 66.40%	100.0	98.14% to 100.0%	
> 97.56	56.31	46.68% to 65.49%	100.0	98.14% to 100.0%	
> 97.58	55.34	45.72% to 64.58%	100.0	98.14% to 100.0%	
> 97.60	54.37	44.77% to 63.66%	100.0	98.14% to 100.0%	
> 97.65	53.40	43.82% to 62.74%	100.0	98.14% to 100.0%	
> 97.71	52.43	42.87% to 61.81%	100.0	98.14% to 100.0%	
> 97.74	51.46	41.93% to 60.88%	100.0	98.14% to 100.0%	
> 97.77	50.49	40.99% to 59.95%	100.0	98.14% to 100.0%	
> 97.82	49.51	40.05% to 59.01%	100.0	98.14% to 100.0%	
> 97.85	48.54	39.12% to 58.07%	100.0	98.14% to 100.0%	
> 97.91	47.57	38.19% to 57.13%	100.0	98.14% to 100.0%	
> 98.04	46.60	37.26% to 56.18%	100.0	98.14% to 100.0%	
> 98.13	45.63	36.34% to 55.23%	100.0	98.14% to 100.0%	
> 98.16	44.66	35.42% to 54.28%	100.0	98.14% to 100.0%	
> 98.24	43.69	34.51% to 53.32%	100.0	98.14% to 100.0%	
> 98.34	42.72	33.60% to 52.36%	100.0	98.14% to 100.0%	
> 98.39	41.75	32.69% to 51.40%	100.0	98.14% to 100.0%	
> 98.43	40.78	31.78% to 50.43%	100.0	98.14% to 100.0%	
> 98.46	39.81	30.88% to 49.46%	100.0	98.14% to 100.0%	
> 98.49	38.83	29.99% to 48.49%	100.0	98.14% to 100.0%	
> 98.51	37.86	29.09% to 47.51%	100.0	98.14% to 100.0%	
> 98.52	35.92	27.32% to 45.54%	100.0	98.14% to 100.0%	
> 98.54	34.95	26.44% to 44.55%	100.0	98.14% to 100.0%	
> 98.56	33.98	25.56% to 43.56%	100.0	98.14% to 100.0%	
> 98.59	33.01	24.68% to 42.56%	100.0	98.14% to 100.0%	
> 98.66	32.04	23.81% to 41.56%	100.0	98.14% to 100.0%	
> 98.75	31.07	22.95% to 40.55%	100.0	98.14% to 100.0%	
> 98.78	30.10	22.09% to 39.54%	100.0	98.14% to 100.0%	
> 98.79	27.18	19.53% to 36.48%	100.0	98.14% to 100.0%	
> 98.82	26.21	18.69% to 35.45%	100.0	98.14% to 100.0%	
> 98.90	25.24	17.85% to 34.42%	100.0	98.14% to 100.0%	
> 98.95	24.27	17.02% to 33.38%	100.0	98.14% to 100.0%	
> 98.98	23.30	16.19% to 32.33%	100.0	98.14% to 100.0%	
> 99.02	22.33	15.37% to 31.28%	100.0	98.14% to 100.0%	
> 99.05	20.39	13.74% to 29.17%	100.0	98.14% to 100.0%	
> 99.08	19.42	12.94% to 28.10%	100.0	98.14% to 100.0%	
> 99.09	18.45	12.14% to 27.02%	100.0	98.14% to 100.0%	
> 99.11	16.50	10.57% to 24.85%	100.0	98.14% to 100.0%	
> 99.14	15.53	9.794% to 23.75%	100.0	98.14% to 100.0%	
> 99.18	14.56	9.028% to 22.65%	100.0	98.14% to 100.0%	
> 99.21	13.59	8.272% to 21.53%	100.0	98.14% to 100.0%	
> 99.26	12.62	7.526% to 20.40%	100.0	98.14% to 100.0%	
> 99.30	10.68	6.069% to 18.12%	100.0	98.14% to 100.0%	
> 99.31	9.709	5.359% to 16.96%	100.0	98.14% to 100.0%	
> 99.33	7.767	3.988% to 14.58%	100.0	98.14% to 100.0%	
> 99.35	6.796	3.331% to 13.37%	100.0	98.14% to 100.0%	
> 99.38	4.854	2.091% to 10.86%	100.0	98.14% to 100.0%	
> 99.39	3.883	1.520% to 9.563%	100.0	98.14% to 100.0%	
> 99.46	2.913	0.7939% to 8.216%	100.0	98.14% to 100.0%	

> 99.56	1.942	0.3450% to 6.805%	100.0	98.14% to 100.0%	
> 99.61	0.9709	0.04980% to 5.296%	100.0	98.14% to 100.0%	

Abbreviations: CI: Confidence Interval.

S3. Calculated EC_{50} values for WT/Delta-sVNT pre and post-vaccination samples

WT EC_{50}				Delta EC_{50}			
Pre-Vaccination	**EC_{50}**	**Post-Vaccination**	**EC_{50}**	**Pre-Vaccination**	**EC_{50}**	**Post-Vaccination**	**EC_{50}**
P126-S00-1005	**NT**	**P126-S00-1005**	**531.5**	**P126-S00-1005**	**NT**	**P126-S00-1005**	**326.1**
P126-S00-1007	**NT**	**P126-S00-1007**	**292.3**	**P126-S00-1007**	**25.65**	**P126-S00-1007**	**253.8**
P126-S00-1008	**NT**	**P126-S00-1008**	**91.97**	**P126-S00-1008**	**NT**	**P126-S00-1008**	**81.51**
P126-S00-1009	**NT**	**P126-S00-1009**	**378**	**P126-S00-1009**	**NT**	**P126-S00-1009**	**245.3**
P126-S00-1011	**165.2**	**P126-S00-1011**	**300.7**	**P126-S00-1011**	**NT**	**P126-S00-1011**	**218.9**
P126-S00-1012	**NT**	**P126-S00-1012**	**160.2**	**P126-S00-1012**	**34.47**	**P126-S00-1012**	**125.1**
P126-S00-1013	**NT**	**P126-S00-1013**	**63.33**	**P126-S00-1013**	**NT**	**P126-S00-1013**	**68.76**
P126-S00-1014	**NT**	**P126-S00-1014**	**125.8**	**P126-S00-1014**	**NT**	**P126-S00-1014**	**116.3**
P126-S00-1015	**NT**	**P126-S00-1015**	**103.9**	**P126-S00-1015**	**NT**	**P126-S00-1015**	**72.88**
P126-S00-1017	**NT**	**P126-S00-1017**	**395.9**	**P126-S00-1017**	**NT**	**P126-S00-1017**	**236.7**
P126-S00-1018	**NT**	**P126-S00-1018**	**360.7**	**P126-S00-1018**	**NT**	**P126-S00-1018**	**295.8**
P126-S00-1020	**NT**	**P126-S00-1020**	**103.2**	**P126-S00-1020**	**NT**	**P126-S00-1020**	**62.06**
P126-S00-1021	**NT**	**P126-S00-1021**	**543.3**	**P126-S00-1021**	**NT**	**P126-S00-1021**	**421.3**
P126-S00-1022	**NT**	**P126-S00-1022**	**131**	**P126-S00-1022**	**NT**	**P126-S00-1022**	**124.1**
P126-S00-1023	**NT**	**P126-S00-1023**	**147.1**	**P126-S00-1023**	**NT**	**P126-S00-1023**	**112**
P126-S00-1024	**NT**	**P126-S00-1024**	**257.1**	**P126-S00-1024**	**NT**	**P126-S00-1024**	**159.2**
P126-S00-1026	**NT**	**P126-S00-1026**	**118.6**	**P126-S00-1026**	**28.38**	**P126-S00-1026**	**79.71**
P126-S00-1027	**241**	**P126-S00-1027**	**70.79**	**P126-S00-1027**	**NT**	**P126-S00-1027**	**55.97**
P126-S00-1029	**NT**	**P126-S00-1029**	**253.1**	**P126-S00-1029**	**NT**	**P126-S00-1029**	**188.9**
P126-S00-1031	**NT**	**P126-S00-1031**	**130.7**	**P126-S00-1031**	**NT**	**P126-S00-1031**	**109.9**
P126-S00-1032	**63.93**	**P126-S00-1032**	**84.62**	**P126-S00-1032**	**NT**	**P126-S00-1032**	**75.55**
P126-S00-1033	**36.57**	**P126-S00-1033**	**148.4**	**P126-S00-1033**	**17.15**	**P126-S00-1033**	**NT**
P126-S00-1037	**NT**	**P126-S00-1037**	**222.1**	**P126-S00-1037**	**NT**	**P126-S00-1037**	**183.1**
P126-S00-1038	**NT**	**P126-S00-1038**	**283.3**	**P126-S00-1038**	**NT**	**P126-S00-1038**	**228.8**
P126-S00-1040	**NT**	**P126-S00-1040**	**110.6**	**P126-S00-1040**	**NT**	**P126-S00-1040**	**75.52**
P126-S00-1041	**NT**	**P126-S00-1041**	**217.3**	**P126-S00-1041**	**NT**	**P126-S00-1041**	**176.2**
P126-S00-1042	**NT**	**P126-S00-1042**	**127.6**	**P126-S00-1042**	**NT**	**P126-S00-1042**	**113.8**
P126-S00-1043	**NT**	**P126-S00-1043**	**225.1**	**P126-S00-1043**	**103.1**	**P126-S00-1043**	**108.6**
P126-S00-1044	**NT**	**P126-S00-1044**	**44.94**	**P126-S00-1044**	**418.3**	**P126-S00-1044**	**31.32**
P126-S00-1045	**NT**	**P126-S00-1045**	**140.1**	**P126-S00-1045**	**NT**	**P126-S00-1045**	**68.18**
P126-S00-1048	**NT**	**P126-S00-1048**	**153.6**	**P126-S00-1048**	**NT**	**P126-S00-1048**	**108.1**
P126-S00-1049	**NT**	**P126-S00-1049**	**152**	**P126-S00-1049**	**NT**	**P126-S00-1049**	**69.89**
P126-S00-1050	**NT**	**P126-S00-1050**	**19.07**	**P126-S00-1050**	**NT**	**P126-S00-1050**	**29.23**

P126-S00-1054	NT	P126-S00-1054	273.7	P126-S00-1054	38.3	P126-S00-1054	182
P126-S00-1055	NT	P126-S00-1055	400.2	P126-S00-1055	10.21	P126-S00-1055	269.9
P126-S00-1056	NT	P126-S00-1056	93.68	P126-S00-1056	NT	P126-S00-1056	78.98
P126-S00-1057	NT	P126-S00-1057	134	P126-S00-1057	NT	P126-S00-1057	116.6
P126-S00-1058	*NT	P126-S00-1058	108.2	P126-S00-1058	3167	P126-S00-1058	84.76
P126-S00-1060	*NT	P126-S00-1060	125.3	P126-S00-1060	NT	P126-S00-1060	120.1
P126-S00-1064	NT	P126-S00-1064	45.45	P126-S00-1064	NT	P126-S00-1064	10.02
P126-S00-1065	NT	P126-S00-1065	475	P126-S00-1065	NT	P126-S00-1065	310.1
P126-S00-1066	NT	P126-S00-1066	146.5	P126-S00-1066	40.37	P126-S00-1066	101.9
P126-S00-1068	NT	P126-S00-1068	809.3	P126-S00-1068	NT	P126-S00-1068	567.7
P126-S00-1069	NT	P126-S00-1069	81.84	P126-S00-1069	NT	P126-S00-1069	66.93
P126-S00-1071	*NT	P126-S00-1071	397.1	P126-S00-1071	65.61	P126-S00-1071	331.3
P126-S00-1073	NT	P126-S00-1073	233	P126-S00-1073	NT	P126-S00-1073	193.6
P126-S00-1074	NT	P126-S00-1074	347.7	P126-S00-1074	NT	P126-S00-1074	248.3
P126-S00-1076	NT	P126-S00-1076	170.2	P126-S00-1076	NT	P126-S00-1076	151.9
P126-S00-1078	NT	P126-S00-1078	76.92	P126-S00-1078	NT	P126-S00-1078	97.39
P126-S00-1079	NT	P126-S00-1079	74.17	P126-S00-1079	NT	P126-S00-1079	105.7
P126-S00-1082	NT	P126-S00-1082	124.9	P126-S00-1082	47.55	P126-S00-1082	152
P126-S00-1084	*NT	P126-S00-1084	275.6	P126-S00-1084	NT	P126-S00-1084	199.3
P126-S00-1085	NT	P126-S00-1085	199.1	P126-S00-1085	NT	P126-S00-1085	125.7
P126-S00-1087	NT	P126-S00-1087	452.9	P126-S00-1087	NT	P126-S00-1087	294
P126-S00-1091	NT	P126-S00-1091	414.4	P126-S00-1091	NT	P126-S00-1091	382.3
P126-S00-1095	NT	P126-S00-1095	777.4	P126-S00-1095	NT	P126-S00-1095	655.7
P126-S00-1101	*NT	P126-S00-1101	234.8	P126-S00-1101	13.64	P126-S00-1101	245.9
P126-S00-1103	*NT	P126-S00-1103	148.5	P126-S00-1103	NT	P126-S00-1103	123.8
P126-S00-1105	NT	P126-S00-1105	181.2	P126-S00-1105	NT	P126-S00-1105	166.4
P126-S00-1106	NT	P126-S00-1106	151.4	P126-S00-1106	83.83	P126-S00-1106	141.9
P126-S00-1107	NT	P126-S00-1107	145.8	P126-S00-1107	NT	P126-S00-1107	108
P126-S00-1109	NT	P126-S00-1109	332.9	P126-S00-1109	NT	P126-S00-1109	265.7
P126-S00-1110	NT	P126-S00-1110	189.4	P126-S00-1110	NT	P126-S00-1110	170.2
P126-S00-1111	NT	P126-S00-1111	184.4	P126-S00-1111	22.73	P126-S00-1111	169.9
P126-S00-1113	NT	P126-S00-1113	151	P126-S00-1113	NT	P126-S00-1113	112.1
P126-S00-1114	NT	P126-S00-1114	171.2	P126-S00-1114	NT	P126-S00-1114	136.9
P126-S00-1115	NT	P126-S00-1115	45.47	P126-S00-1115	*NT	P126-S00-1115	29.95
P126-S00-1116	NT	P126-S00-1116	404	P126-S00-1116	NT	P126-S00-1116	295.9
P126-S00-1118	NT	P126-S00-1118	226.5	P126-S00-1118	NT	P126-S00-1118	214.5
P126-S00-1119	NT	P126-S00-1119	177	P126-S00-1119	NT	P126-S00-1119	100.3
P126-S00-1120	NT	P126-S00-1120	199.7	P126-S00-1120	NT	P126-S00-1120	154.8
P126-S00-1126	NT	P126-S00-1126	99.35	P126-S00-1126	*NT	P126-S00-1126	83.14
P126-S00-1130	NT	P126-S00-1130	403.5	P126-S00-1130	NT	P126-S00-1130	229.6

P126-S00-1134	NT	P126-S00-1134	293.2	P126-S00-1134	NT	P126-S00-1134	216.4
P126-S00-1135	NT	P126-S00-1135	269.1	P126-S00-1135	37.57	P126-S00-1135	208.2
P126-S00-1136	NT	P126-S00-1136	77.96	P126-S00-1136	*NT	P126-S00-1136	73.21
P126-S00-1137	NT	P126-S00-1137	339.2	P126-S00-1137	*NT	P126-S00-1137	230.1
P126-S00-1142	25.07	P126-S00-1142	444.6	P126-S00-1142	32.53	P126-S00-1142	381.3
P126-S00-1143	NT	P126-S00-1143	144.9	P126-S00-1143	NT	P126-S00-1143	118.7
P126-S00-1146	NT	P126-S00-1146	42.78	P126-S00-1146	*NT	P126-S00-1146	45.47
P126-S00-1149	NT	P126-S00-1149	96.44	P126-S00-1149	NT	P126-S00-1149	86.93
P126-S00-1150	NT	P126-S00-1150	285.4	P126-S00-1150	NT	P126-S00-1150	167.2
P126-S00-1152	NT	P126-S00-1152	168.1	P126-S00-1152	*NT	P126-S00-1152	164.1
P126-S00-1153	*NT	P126-S00-1153	319.6	P126-S00-1153	NT	P126-S00-1153	277.4
P126-S00-1154	****	P126-S00-1154	502.3	P126-S00-1154	NT	P126-S00-1154	401.3
P126-S00-1155	NT	P126-S00-1155	131.6	P126-S00-1155	NT	P126-S00-1155	113.9
P126-S00-1156	NT	P126-S00-1156	133.5	P126-S00-1156	NT	P126-S00-1156	118.4
P126-S00-1157	NT	P126-S00-1157	247.6	P126-S00-1157	NT	P126-S00-1157	213.2
P126-S00-1160	NT	P126-S00-1160	64.3	P126-S00-1160	NT	P126-S00-1160	63.22
P126-S00-1161	NT	P126-S00-1161	112.9	P126-S00-1161	***	P126-S00-1161	106.6
P126-S00-1162	NT	P126-S00-1162	189.4	P126-S00-1162	NT	P126-S00-1162	189.4
P126-S00-1163	NT	P126-S00-1163	133.7	P126-S00-1163	1.14E+14	P126-S00-1163	108.2
P126-S00-1165	NT	P126-S00-1165	59.11	P126-S00-1165	NT	P126-S00-1165	44.37
P126-S00-1168	1402	P126-S00-1168	302	P126-S00-1168	NT	P126-S00-1168	226.8
P126-S00-1169	NT	P126-S00-1169	22.4	P126-S00-1169	1568	P126-S00-1169	30.91
P126-S00-1170	308.4	P126-S00-1170	276.9	P126-S00-1170	NT	P126-S00-1170	258.1
P126-S00-1172	NT	P126-S00-1172	77.7	P126-S00-1172	NT	P126-S00-1172	44.32
P126-S00-1173	NT	P126-S00-1173	276.5	P126-S00-1173	NT	P126-S00-1173	293
P126-S00-1175	282.9	P126-S00-1175	98.13	P126-S00-1175	NT	P126-S00-1175	62.5
P126-S00-1177	1169	P126-S00-1177	31.09	P126-S00-1177	NT	P126-S00-1177	32.05
P126-S00-1178	NT	P126-S00-1178	119.4	P126-S00-1178	1697	P126-S00-1178	82.33
P126-S00-1179	NT	P126-S00-1179	239.9	P126-S00-1179	NT	P126-S00-1179	203.1
P126-S00-1180	NT	P126-S00-1180	229.2	P126-S00-1180	NT	P126-S00-1180	160.9

NT- Not determined; defined in GraphPad as ambiguous and unable to find a unique fit to the data; most likely due to pre-vaccination samples have low to no antibody response.
*NT- interrupted most likely due to the data not having enough information for the model to fit.
Abbreviations: EC_{50}: Half-maximal effective concentration; WT/Delta sVNT: Wild Type/Delta –surrogate virus neutraliztion test; NT: Not Determined; *NT: Interupted; ***: Not converged.

S4. Calculated EC_{80} values for WT/Delta-sVNT pre and post-vaccination samples

WT EC_{80}			Delta EC_{80}				
Pre-Vaccination	EC_{80}	Post-Vaccination	EC_{80}	Pre-Vaccination	EC_{80}	Post-Vaccination	EC_{80}
P126-S00-1005	NT	P126-S00-1005	190.8	P126-S00-1005	NT	P126-S00-1005	129.5
P126-S00-1007	NT	P126-S00-1007	102.7	P126-S00-1007	4.569	P126-S00-1007	82.4
P126-S00-1008	NT	P126-S00-1008	26.72	P126-S00-1008	NT	P126-S00-1008	30.78
P126-S00-1009	NT	P126-S00-1009	133.8	P126-S00-1009	NT	P126-S00-1009	107.2
P126-S00-1011	68.3	P126-S00-1011	126.3	P126-S00-1011	NT	P126-S00-1011	65.51
P126-S00-1012	NT	P126-S00-1012	56.33	P126-S00-1012	NT	P126-S00-1012	45.28
P126-S00-1013	NT	P126-S00-1013	21.84	P126-S00-1013	NT	P126-S00-1013	22.38
P126-S00-1014	NT	P126-S00-1014	42.32	P126-S00-1014	NT	P126-S00-1014	33.92
P126-S00-1015	NT	P126-S00-1015	37.99	P126-S00-1015	NT	P126-S00-1015	23.37
P126-S00-1017	NT	P126-S00-1017	103.9	P126-S00-1017	NT	P126-S00-1017	87.58
P126-S00-1018	NT	P126-S00-1018	140	P126-S00-1018	NT	P126-S00-1018	94
P126-S00-1020	NT	P126-S00-1020	24.29	P126-S00-1020	NT	P126-S00-1020	17.72
P126-S00-1021	NT	P126-S00-1021	235.9	P126-S00-1021	NT	P126-S00-1021	130.8
P126-S00-1022	NT	P126-S00-1022	72.69	P126-S00-1022	NT	P126-S00-1022	46.7
P126-S00-1023	NT	P126-S00-1023	51.53	P126-S00-1023	NT	P126-S00-1023	42.39
P126-S00-1024	NT	P126-S00-1024	84.94	P126-S00-1024	NT	P126-S00-1024	67.03
P126-S00-1026	*NT	P126-S00-1026	46.74	P126-S00-1026	19.37	P126-S00-1026	29.08
P126-S00-1027	55.92	P126-S00-1027	21.01	P126-S00-1027	NT	P126-S00-1027	17.16
P126-S00-1029	NT	P126-S00-1029	100.3	P126-S00-1029	NT	P126-S00-1029	53.03
P126-S00-1031	NT	P126-S00-1031	32.25	P126-S00-1031	NT	P126-S00-1031	35.67
P126-S00-1032	39.92	P126-S00-1032	27.55	P126-S00-1032	NT	P126-S00-1032	18.91
P126-S00-1033	3.127	P126-S00-1033	41.75	P126-S00-1033	7.087	P126-S00-1033	NT
P126-S00-1037	NT	P126-S00-1037	72.32	P126-S00-1037	NT	P126-S00-1037	54.56
P126-S00-1038	NT	P126-S00-1038	97.4	P126-S00-1038	NT	P126-S00-1038	65.22
P126-S00-1040	NT	P126-S00-1040	35.97	P126-S00-1040	NT	P126-S00-1040	23.99
P126-S00-1041	NT	P126-S00-1041	76.79	P126-S00-1041	NT	P126-S00-1041	51.77
P126-S00-1042	NT	P126-S00-1042	48.18	P126-S00-1042	NT	P126-S00-1042	40.81
P126-S00-1043	46.66	P126-S00-1043	104.1	P126-S00-1043	38.82	P126-S00-1043	64.35
P126-S00-1044	NT	P126-S00-1044	12.12	P126-S00-1044	23.79	P126-S00-1044	20.53
P126-S00-1045	NT	P126-S00-1045	31.72	P126-S00-1045	NT	P126-S00-1045	35.85
P126-S00-1048	NT	P126-S00-1048	46.07	P126-S00-1048	NT	P126-S00-1048	31.74
P126-S00-1049	NT	P126-S00-1049	56.03	P126-S00-1049	NT	P126-S00-1049	21.96
P126-S00-1050	NT	P126-S00-1050	3.121	P126-S00-1050	NT	P126-S00-1050	7.835
P126-S00-1054	NT	P126-S00-1054	99.83	P126-S00-1054	11.13	P126-S00-1054	61.62
P126-S00-1055	NT	P126-S00-1055	128	P126-S00-1055	1.943	P126-S00-1055	117.6
P126-S00-1056	NT	P126-S00-1056	31.23	P126-S00-1056	8.022E-09	P126-S00-1056	25.99
P126-S00-1057	NT	P126-S00-1057	50.03	P126-S00-1057	NT	P126-S00-1057	41.02
P126-S00-1058	*NT	P126-S00-1058	46.15	P126-S00-1058	7014	P126-S00-1058	30.2
P126-S00-1060	*NT	P126-S00-1060	37.66	P126-S00-1060	NT	P126-S00-1060	44.84

P126-S00-1064	NT	P126-S00-1064	18.96	P126-S00-1064	NT	P126-S00-1064	1.171
P126-S00-1065	NT	P126-S00-1065	160.5	P126-S00-1065	*NT	P126-S00-1065	95.93
P126-S00-1066	NT	P126-S00-1066	49.15	P126-S00-1066	14.6	P126-S00-1066	30.21
P126-S00-1068	NT	P126-S00-1068	249.1	P126-S00-1068	NT	P126-S00-1068	207.4
P126-S00-1069	NT	P126-S00-1069	22.75	P126-S00-1069	NT	P126-S00-1069	22.3
P126-S00-1071	*NT	P126-S00-1071	142.9	P126-S00-1071	2.056	P126-S00-1071	132.9
P126-S00-1073	NT	P126-S00-1073	65.54	P126-S00-1073	NT	P126-S00-1073	66.03
P126-S00-1074	*NT	P126-S00-1074	136.1	P126-S00-1074	NT	P126-S00-1074	77.21
P126-S00-1076	NT	P126-S00-1076	54.03	P126-S00-1076	NT	P126-S00-1076	41.96
P126-S00-1078	NT	P126-S00-1078	39.51	P126-S00-1078	NT	P126-S00-1078	24.34
P126-S00-1079	NT	P126-S00-1079	38.89	P126-S00-1079	NT	P126-S00-1079	33.06
P126-S00-1082	NT	P126-S00-1082	66.68	P126-S00-1082	12.61	P126-S00-1082	49.4
P126-S00-1084	*NT	P126-S00-1084	105.4	P126-S00-1084	NT	P126-S00-1084	52.02
P126-S00-1085	NT	P126-S00-1085	53.09	P126-S00-1085	NT	P126-S00-1085	37.28
P126-S00-1087	NT	P126-S00-1087	148.7	P126-S00-1087	NT	P126-S00-1087	89.46
P126-S00-1091	NT	P126-S00-1091	176.5	P126-S00-1091	NT	P126-S00-1091	128.8
P126-S00-1095	NT	P126-S00-1095	267.1	P126-S00-1095	NT	P126-S00-1095	256.6
P126-S00-1101	*NT	P126-S00-1101	108.2	P126-S00-1101	5.745	P126-S00-1101	73.31
P126-S00-1103	*NT	P126-S00-1103	49.58	P126-S00-1103	NT	P126-S00-1103	38.34
P126-S00-1105	NT	P126-S00-1105	57.72	P126-S00-1105	NT	P126-S00-1105	51.19
P126-S00-1106	NT	P126-S00-1106	62.13	P126-S00-1106	60.93	P126-S00-1106	49.31
P126-S00-1107	NT	P126-S00-1107	45.56	P126-S00-1107	***	P126-S00-1107	34.2
P126-S00-1109	NT	P126-S00-1109	139.3	P126-S00-1109	NT	P126-S00-1109	93.1
P126-S00-1110	NT	P126-S00-1110	70.3	P126-S00-1110	NT	P126-S00-1110	62.74
P126-S00-1111	NT	P126-S00-1111	64.7	P126-S00-1111	4.688	P126-S00-1111	49.24
P126-S00-1113	NT	P126-S00-1113	52.46	P126-S00-1113	NT	P126-S00-1113	38.34
P126-S00-1114	NT	P126-S00-1114	69.52	P126-S00-1114	NT	P126-S00-1114	44.28
P126-S00-1115	NT	P126-S00-1115	11.34	P126-S00-1115	*NT	P126-S00-1115	7.546
P126-S00-1116	NT	P126-S00-1116	119.3	P126-S00-1116	NT	P126-S00-1116	101.7
P126-S00-1118	NT	P126-S00-1118	67.05	P126-S00-1118	NT	P126-S00-1118	61.63
P126-S00-1119	NT	P126-S00-1119	55.71	P126-S00-1119	NT	P126-S00-1119	39.9
P126-S00-1120	NT	P126-S00-1120	75.21	P126-S00-1120	NT	P126-S00-1120	55.24
P126-S00-1126	NT	P126-S00-1126	36.99	P126-S00-1126	*NT	P126-S00-1126	24.87
P126-S00-1130	NT	P126-S00-1130	178.8	P126-S00-1130	479.1	P126-S00-1130	90.9
P126-S00-1134	NT	P126-S00-1134	92.67	P126-S00-1134	NT	P126-S00-1134	68.26
P126-S00-1135	NT	P126-S00-1135	97.23	P126-S00-1135	24.59	P126-S00-1135	73.44
P126-S00-1136	NT	P126-S00-1136	20.42	P126-S00-1136	*NT	P126-S00-1136	22.41
P126-S00-1137	NT	P126-S00-1137	124.4	P126-S00-1137	*NT	P126-S00-1137	80.37
P126-S00-1142	15.38	P126-S00-1142	157.2	P126-S00-1142	5.537	P126-S00-1142	146.7
P126-S00-1143	NT	P126-S00-1143	58.36	P126-S00-1143	NT	P126-S00-1143	38.06
P126-S00-1146	NT	P126-S00-1146	14.59	P126-S00-1146	*NT	P126-S00-1146	12.65
P126-S00-1149	NT	P126-S00-1149	24.73	P126-S00-1149	NT	P126-S00-1149	26.21

P126-S00-1150	NT	P126-S00-1150	112.6	P126-S00-1150	NT	P126-S00-1150	54.05
P126-S00-1152	NT	P126-S00-1152	67.09	P126-S00-1152	*NT	P126-S00-1152	54.34
P126-S00-1153	*NT	P126-S00-1153	103.5	P126-S00-1153	NT	P126-S00-1153	104.7
P126-S00-1154	NT	P126-S00-1154	197.4	P126-S00-1154	NT	P126-S00-1154	157
P126-S00-1155	NT	P126-S00-1155	48.82	P126-S00-1155	NT	P126-S00-1155	34.89
P126-S00-1156	NT	P126-S00-1156	48.2	P126-S00-1156	NT	P126-S00-1156	40.68
P126-S00-1157	NT	P126-S00-1157	89.72	P126-S00-1157	NT	P126-S00-1157	80.44
P126-S00-1160	NT	P126-S00-1160	15.61	P126-S00-1160	NT	P126-S00-1160	20.62
P126-S00-1161	*NT	P126-S00-1161	34.81	P126-S00-1161	NT	P126-S00-1161	27.77
P126-S00-1162	NT	P126-S00-1162	75.07	P126-S00-1162	8.83	P126-S00-1162	40.79
P126-S00-1163	NT	P126-S00-1163	43.34	P126-S00-1163	NT	P126-S00-1163	38.09
P126-S00-1165	NT	P126-S00-1165	17.98	P126-S00-1165	NT	P126-S00-1165	17.53
P126-S00-1168	935.8	P126-S00-1168	101.7	P126-S00-1168	NT	P126-S00-1168	83.34
P126-S00-1169	NT	P126-S00-1169	6.273	P126-S00-1169	NT	P126-S00-1169	12.88
P126-S00-1170	355.5	P126-S00-1170	104.3	P126-S00-1170	NT	P126-S00-1170	102.7
P126-S00-1172	NT	P126-S00-1172	26.42	P126-S00-1172	NT	P126-S00-1172	15.02
P126-S00-1173	NT	P126-S00-1173	78.67	P126-S00-1173	NT	P126-S00-1173	91.48
P126-S00-1175	8.603	P126-S00-1175	33.02	P126-S00-1175	NT	P126-S00-1175	24.3
P126-S00-1177	500	P126-S00-1177	7.575	P126-S00-1177	NT	P126-S00-1177	10.27
P126-S00-1178	NT	P126-S00-1178	39.54	P126-S00-1178	899.3	P126-S00-1178	32.31
P126-S00-1179	NT	P126-S00-1179	92.45	P126-S00-1179	NT	P126-S00-1179	85.1
P126-S00-1180	NT	P126-S00-1180	75.75	P126-S00-1180	NT	P126-S00-1180	58.36

NT- Not determined; defined in GraphPad as ambiguous and unable to find a unique fit to the data; most likely due to pre-vaccination samples have low to no antibody response.
*NT- interrupted most likely due to the data not having enough information for the model to fit.
Abbreviations: EC_{80}: 80% of maximal effective concentration; WT/Delta sVNT: Wild Type/Delta –surrogate virus neutraliztion test; NT: Not Determined; *NT: Interupted; ***: Not converged.

S5. Calculated EC_{50} values for WT-MN and WT/Delta PNA post-vaccination samples

Sample ID	MN EC_{50} WT	PNA EC_{50} WT	PNA EC_{50} Delta
P126-S00-1005	320		
P126-S00-1007	320		
P126-S00-1008	160		
P126-S00-1009	1280	1166	407
P126-S00-1011	320		
P126-S00-1012	160	1341	1462
P126-S00-1013	20	235	120
P126-S00-1014	160		

P126-S00-1015	80		
P126-S00-1017	320		
P126-S00-1018	320	1547	1917
P126-S00-1020	40		
P126-S00-1021	320	1561	502
P126-S00-1022	320		
P126-S00-1023	160		
P126-S00-1024	160		
P126-S00-1026	160	389	122
P126-S00-1027	40	299	114
P126-S00-1029	80	1055	569
P126-S00-1031	80	636	694
P126-S00-1032	40	246	314
P126-S00-1033	320		
P126-S00-1037	160	673	325
P126-S00-1038	160	825	385
P126-S00-1039		531	345
P126-S00-1040	160		
P126-S00-1041	320		
P126-S00-1042	160		
P126-S00-1043	80	903	363
P126-S00-1044	40		
P126-S00-1045	80		
P126-S00-1048	160	725	283
P126-S00-1049	40		
P126-S00-1050	40		
P126-S00-1054	160		
P126-S00-1055	640		
P126-S00-1056	80		
P126-S00-1057	1280		
P126-S00-1058	160		
P126-S00-1060	40	347	135
P126-S00-1064	80	360	119
P126-S00-1065	640		
P126-S00-1066	320		
P126-S00-1068	640		
P126-S00-1069	160		
P126-S00-1071	640		
P126-S00-1073	160		
P126-S00-1074	320	1034	492

P126-S00-1076	160	787	461
P126-S00-1078	80	527	282
P126-S00-1079	160	324	200
P126-S00-1082	160	695	314
P126-S00-1084	160		
P126-S00-1085	40		
P126-S00-1087	320		
P126-S00-1091	320		
P126-S00-1095	1280		
P126-S00-1101	160		
P126-S00-1103	80	478	216
P126-S00-1105	160		
P126-S00-1106	160		
P126-S00-1107	160		
P126-S00-1109	640		
P126-S00-1110	640		
P126-S00-1111	160		
P126-S00-1113	320	406	257
P126-S00-1114	160		
P126-S00-1115	40		
P126-S00-1116	320		
P126-S00-1118	160		
P126-S00-1119	80		
P126-S00-1120	160		
P126-S00-1126	40	474	723
P126-S00-1130	160		
P126-S00-1134	160	593	222
P126-S00-1135	160		
P126-S00-1136	80		
P126-S00-1137	320	3284	729
P126-S00-1142	320		
P126-S00-1143	160	369	148
P126-S00-1146	40		
P126-S00-1149	80		
P126-S00-1150	160	756	447
P126-S00-1152	160		
P126-S00-1153	320	942	223
P126-S00-1154	640	1400	800
P126-S00-1155	160	386	226
P126-S00-1156	80	367	230

P126-S00-1157	320		
P126-S00-1160	40	156	62
P126-S00-1161	80		
P126-S00-1162	320		
P126-S00-1163	160		
P126-S00-1165	80		
P126-S00-1166		610	402
P126-S00-1168	320		
P126-S00-1169	20		
P126-S00-1170	160		
P126-S00-1172	160	239	55
P126-S00-1173	160	558	395
P126-S00-1175	320		
P126-S00-1177	80		
P126-S00-1178	160		
P126-S00-1179	80		
P126-S00-1180	610	468	164

Abbreviations: EC_{50}: Half-maximal effective concentration; WT-MN: Wild Type – micronuetralization assay; WT/Delta PNA: Wild Type/Delta –pseudovirus neutraliztion assay.

REFERENCES

Aldo P, Marusov G, Svancara D, David J, Mor G. 2016. Simple Plex TM : A Novel Multi-Analyte, Automated Microfluidic Immunoassay Platform for the Detection of Human and Mouse Cytokines and Chemokines. American Journal of Reproductive Immunology. 75(6):678–693. doi:10.1111/aji.12512.

Amanat F, Stadlbauer D, Strohmeier S, Nguyen THO, Chromikova V, McMahon M, Jiang K, Arunkumar GA, Jurczyszak D, Polanco J, et al. 2020 Mar 18. A serological assay to detect SARS-CoV-2 seroconversion in humans. doi:10.1101/2020.03.17.20037713.

Bewley KR, Coombes NS, Gagnon L, McInroy L, Baker N, Shaik I, St-Jean JR, St-Amant N, Buttigieg KR, Humphries HE, et al. 2021. Quantification of SARS-CoV-2 neutralizing antibody by wild-type plaque reduction neutralization, microneutralization and pseudotyped virus neutralization assays. Nature Protocols. 16(6):3114–3140. doi:10.1038/s41596-021-00536-y. https://www.nature.com/articles/s41596-021-00536-y.

Brown EEF, Rezaei R, Jamieson TR, Dave J, Martin NT, Singaravelu R, Crupi MJF, Boulton S, Tucker S, Duong J, et al. 2021. Characterization of Critical Determinants of ACE2–SARS CoV-2 RBD Interaction. International Journal of Molecular Sciences. 22(5):2268. doi:10.3390/ijms22052268.

Chen X, Bailleux F, Desai K, Qin L, Dunning AJ. 2013. A threshold method for immunological correlates of protection. BMC Medical Research Methodology. 13(1). doi:10.1186/1471-2288-13-29.

Coggins SA, Laing ED, Olsen CH, Goguet E, Moser M, Jackson-Thompson BM, Samuels EC, Pollett SD, Tribble DR, Davies J, et al. Adverse effects and antibody titers in response to the BNT162b2 mRNA COVID-19 vaccine in a prospective study of healthcare workers. Open forum infectious diseases. 2022;9(1):ofab575. http://dx.doi.org/10.1093/ofid/ofab575. doi:10.1093/ofid/ofab575

Coronavirus (COVID-19) update: FDA authorizes first test that detects neutralizing antibodies from recent or prior SARS-CoV-2 infection. 2020 Nov 6. FDA. [accessed 2021 Dec 10]. https://www.fda.gov/news-events/press-announcements/coronavirus-covid-19-update-fda-authorizes-first-test-detects-neutralizing-antibodies-recent-or.

COVID-19: SARS-CoV-2 variant classifications and definitions. 2020 Feb 11. Centers for Disease Control and Prevention. [accessed 2021 Dec 10]. https://www.cdc.gov/coronavirus/2019-ncov/variants/variant-classifications.html#anchor_1632154493691.

Crawford KHD, Eguia R, Dingens AS, Loes AN, Malone KD, Wolf CR, Chu HY, Tortorici MA, Veesler D, Murphy M, et al. 2020. Protocol and Reagents for Pseudotyping Lentiviral Particles with SARS-CoV-2 Spike Protein for Neutralization

Assays. Viruses. 12(5):513. doi:10.3390/v12050513. [accessed 2022 Mar 25]. https://www.ncbi.nlm.nih.gov/pmc/articles/PMC7291041/.

Customizable assays on Ella. Bio-Techne ProteinSimple. 2022. [accessed 2022 Feb 11]. https://www.proteinsimple.com/ella-customizable-assays.html.

Day MJ. 2015. Introduction to Antigen and Antibody Assays. Topics in Companion Animal Medicine. 30(4):128–131. doi:10.1053/j.tcam.2015.12.001.

Du L, Yang Y, Zhang X. 2021 Sep 8. Neutralizing antibodies for the prevention and treatment of COVID-19. Cellular & Molecular Immunology. doi:10.1038/s41423-021-00752-2.

Ella. Your immunoassay problem solver. 2017. Bio-Techne ProteinSimple. [accessed 2021 Nov 5]. https://www.proteinsimple.com/documents/Ella_brochure_RevF.PDF?_ga=2.218253017.1361235658.1636652143-1395936625.1636652143.

Feng S, Phillips DJ, White T, Sayal H, Aley PK, Bibi S, Dold C, Fuskova M, Gilbert SC, Hirsch I, et al. 2021. Correlates of protection against symptomatic and asymptomatic SARS-CoV-2 infection. Nature Medicine. 27(11):2032–2040. doi:10.1038/s41591-021-01540-1.

Ghaffari A, Meurant R, Ardakani A. 2020. COVID-19 Serological Tests: How Well Do They Actually Perform? Diagnostics. 10(7):453. doi:10.3390/diagnostics10070453.

Goher SS, Ali F, Amin M. 2021 Dec. The Delta Variant Mutations in the Receptor Binding Domain of SARS-CoV-2 Show Enhanced Electrostatic Interactions with the ACE2. Medicine in Drug Discovery.:100114. doi:10.1016/j.medidd.2021.100114.

Hofmann N, Grossegesse M, Neumann M, Schaade L, Nitsche A. 2022. Evaluation of a commercial ELISA as alternative to plaque reduction neutralization test to detect neutralizing antibodies against SARS-CoV-2. Scientific Reports. 12(1). doi:10.1038/s41598-022-07597-3.

Huang Y, Yang C, Xu X, Xu W, Liu S. 2020. Structural and functional properties of SARS-CoV-2 spike protein: potential antivirus drug development for COVID-19. Acta Pharmacologica Sinica. 41(9):1141–1149. doi:10.1038/s41401-020-0485-4.

Jain S, Batra H, Yadav P, Chand S. 2020. COVID-19 Vaccines Currently under Preclinical and Clinical Studies, and Associated Antiviral Immune Response. Vaccines. 8(4):649. doi:10.3390/vaccines8040649.

Krammer F. 2021. A correlate of protection for SARS-CoV-2 vaccines is urgently needed. Nature Medicine. 27(7):1147–1148. doi:10.1038/s41591-021-01432-4. [accessed 2021 Jul 21]. https://www.nature.com/articles/s41591-021-01432-4.

Labant M. 2016 Nov 28. Developing Biomarkers for Improved Therapeutics. GEN - Genetic Engineering and Biotechnology News. [accessed 2021 Nov 8]. https://www.genengnews.com/magazine/283/supplement-developing-biomarkers-for-improved-therapeutics/.

Lu Y, Wang J, Li Q, Hu H, Lu J, Chen Z. 2021. Advances in Neutralization Assays for SARS-CoV-2. Scandinavian Journal of Immunology. 94(3). doi:10.1111/sji.13088.

Luo YR, Yun C, Chakraborty I, Wu AHB, Lynch KL. 2021. A SARS-CoV-2 Label-Free Surrogate Virus Neutralization Test and a Longitudinal Study of Antibody Characteristics in COVID-19 Patients. Tang Y-W, editor. Journal of Clinical Microbiology. 59(7). doi:10.1128/jcm.00193-21.

Pang NY-L, Pang AS-R, Chow VT, Wang D-Y. 2021. Understanding neutralising antibodies against SARS-CoV-2 and their implications in clinical practice. Military Medical Research. 8(1). doi:10.1186/s40779-021-00342-3.

Payne S. 2017 Jan 1. Chapter 6 - Immunity and Resistance to Viruses. Payne S, editor. ScienceDirect.:61–71. https://www.sciencedirect.com/science/article/pii/B9780128031094000064.

Pseudovirus neutralization assays in SARS-CoV-2 research. 2021. Berthold Technologies GmbH & Co.KG. [accessed 2021 Dec 13]. https://www.berthold.com/en-us/bioanalytic/solutions-that-support-your-sars-cov-2-covid-19-research/pseudovirus-neutralization-assays-in-sars-cov-2-research/.

Simple Plex Assays - Human, mouse and rat analytes. 2021 Nov 23. Bio-Techne ProteinSimple. [accessed 2021 Nov 23]. https://proteinsimple.com/simple_plex_assays.html.

Sternberg A, Naujokat C. 2020 Jul. Structural features of coronavirus SARS-CoV-2 spike protein: Targets for vaccination. Life Sciences.:118056. doi:10.1016/j.lfs.2020.118056.

Steward K. 2021 Mar 24. Leveraging Pseudoviruses in the Face of the COVID-19 Pandemic. Immunology and Microbiology. [accessed 2021 Nov 5]. https://www.technologynetworks.com/immunology/articles/leveraging-pseudoviruses-in-the-face-of-the-covid-19-pandemic-347021.

Tan CW, Chia WN, Qin X, Liu P, Chen MI-C ., Tiu C, Hu Z, Chen VC-W, Young BE, Sia WR, et al. 2020. A SARS-CoV-2 surrogate virus neutralization test based on antibody-mediated blockage of ACE2–spike protein–protein interaction. Nature Biotechnology. 38(9):1073–1078. doi:10.1038/s41587-020-0631-z. https://www.nature.com/articles/s41587-020-0631-z.

Valcourt EJ, Manguiat K, Robinson A, Chen JC-Y, Dimitrova K, Philipson C, Lamoureux L, McLachlan E, Schiffman Z, Drebot MA, et al. 2021. Evaluation of a commercially-available surrogate virus neutralization test for severe acute respiratory

syndrome coronavirus-2 (SARS-CoV-2). Diagnostic Microbiology and Infectious Disease. 99(4):115294. doi:10.1016/j.diagmicrobio.2020.115294. [accessed 2021 Nov 26]. https://www.sciencedirect.com/science/article/pii/S0732889320306714.

von Rhein C, Scholz T, Henss L, Kronstein-Wiedemann R, Schwarz T, Rodionov RN, Corman VM, Tonn T, Schnierle BS. 2021. Comparison of potency assays to assess SARS-CoV-2 neutralizing antibody capacity in COVID-19 convalescent plasma. Journal of Virological Methods. 288:114031. doi:10.1016/j.jviromet.2020.114031.